

## **Response to reviews of Pilch Kedzierski et al.: “Wave Modulation of the Extratropical Tropopause Inversion Layer”**

Dear Editor,

We would like to thank the three reviewers and A. P. Ferreira for their helpful comments. The manuscript has benefited greatly from their suggestions, especially in the more detailed description of our filtering method, the wave modulation mechanism, and the discussion section linking it to previous literature. The manuscript has gained length significantly, but we feel that it has also gained in clarity and integration within TIL literature.

In the following paragraphs we include our point-by-point response to each comment in the reviews along with the changes made in the manuscript. The referee's comments are in **blue font**, and our replies are in normal font. Every change made in the revised manuscript is **highlighted**. We hope that the new version fulfills the reviewer's requests.

Yours sincerely,

Robin Pilch Kedzierski  
Katja Matthes  
Karl Bumke

### **General comments**

Taking into account all comments, we realized that most of them are grouped around two main issues:

1) The filtering method and the wave modulation mechanism. These needed more detailed explanations, which have been expanded. Especially regarding our wave modulation mechanism, we added two panels to Figure 2 (b and c now), and we separated the explanation of the mechanism into a new subsection 2.4 (it was part of subsection “2.3: Wavenumber-frequency domain filtering” before).

2) The interpretation of our results and their relation to earlier studies and previously proposed mechanisms. In the submitted manuscript we did not discuss this, and we agree with the comments that our paper would benefit greatly from such discussion. Now, we created a new discussion section 5, linking the wave modulation mechanism to isentrope packing above anticyclones (Wirth 2003, 2004), wave breaking (Erler and Wirth 2011) and radiative effects from water vapor / clouds (Miyazaki 2010, Kunkel et al. 2016, Ferreira et al. 2016). In this

detailed discussion we suggest that all these mechanisms, directly or indirectly, can integrate into the amplified extratropical wave whose effect is adiabatic and transient. In our opinion, the important benefit of our method is that it separates this transient effect, as defined with space-time harmonics of T and N2 anomalies whose sum is zero in the ground-based mean, from the rest. The diabatic and irreversible processes from radiation and residual circulation, and their direct influence on the TIL, are still present in Figs. 7b and 9b once our wave anomalies are subtracted.

We stress that ultimately the direct effect on the TIL is done by extratropical waves (see the new section 5 for the detailed discussion) in an adiabatic and transient way, and the remaining question is what causes the waves to gain large amplitudes. We suggest that some process, possibly a radiative-dynamical feedback, is helping wave growth near the tropopause

## **Point-by-point responses to Ref#1**

### **Specific comments (major)**

#### **1. For filtering method and their physical interpretation:**

Authors are using filtering limits of 2-4, 4-25, 30-96 days in time and -10 to 10 wavenumber in zonal direction. The choice of filter domain is subjective, and it is difficult to make a physical connection between the filter area and mid/high latitude waves. The filter seems to cover too broad spectral range, and it may remove most of the variability within 2-96 days. Particularly, the TIL could be easily removed by variation in tropopause height, because the TIL is defined in tropopause-relative coordinate and filtering is made in altitude coordinate. Therefore, a large portion of the “tropopause-based zonal-mean TIL (shown in Figs. 5, 7, and 9)” could be filtered out, NOT because it is a part of Rossby waves BUT because Rossby waves simply change height of the tropopause. This problem could be worse with a large filter area, and authors may want to test this issue.

We added several additional paragraphs throughout subsections 2.3 and the new 2.4 in order to clarify the filtering method, why it is optimal for the purpose of this study, and how the wave modulation mechanism works. No filtering is done in the vertical dimension, each vertical level is filtered separately (the filters work with longitude-time arrays, see subsection 2.2).

Rossby waves (and other types) modulate the T and N2 structures around the tropopause, changing the tropopause height and enhancing the TIL: there is no chain of causality here, it all happens simultaneously and only due to the presence of the wave. Apart from the increased detail in subsections 2.3 and 2.4, we further discuss the interpretation of our results in the new section 5.

We stress that the choosing of a broad spectral range is in order to capture as much wave variability as possible. If waves are not present, they won't have any effect on the tropopause-based means (l. 259-264), so a broader and partly empty spectral range is not a disadvantage.

Also note that, after subtracting the wave signal (see Figs. 7b and 9b), the remaining TIL and its timing with processes that are more permanent and irreversible (accelerated residual circulation during SSWs, and radiative effects from water vapor in polar summer) is in very good agreement with previous TIL literature.

I agree with authors that it is difficult to define general filter area (or filtering method) for mid-latitude waves. However, some efforts are still required to define reasonable filtering area in order to overcome the limitation and get more reliable results. Careful examination on wavenumber-frequency spectrums may be helpful for figuring out Rossy wave signature in the TIL, and some results of it will also be appreciated by readership.

We now added several paragraphs throughout subsections 2.3 and 2.4 (new) explaining more in detail why our filtering method is optimal for the purpose of the study. Regarding the detailed examination of the extratropical wave spectrum: this implies a similar study as Wheeler and Kiladis (1999), an update for the extratropics. Such study would itself yield a separate and abundant paper, and is well beyond the scope of the present manuscript that focuses on the TIL and its formation mechanisms; not on particular properties of atmospheric waves.

Minor note:

Authors mentioned that they “define a seventh filter for wavenumber zero for completeness (page 7, line 229)”. It sounds like “the filter used for Figs. 5, 7 and 9 also removes wavenumber zero along with wavenumber 1-10”. If this is the case, wavenumber zero should not be filtered as it is a part of mean overturning circulation (i.e., deep or shallow branch of the Brewer-Dobson circulation).

The  $s=0$  filter represents zonally-symmetric, annular oscillations in time (any possible pole-trapped wave mode). We include this now in line 245-246 . Note that for a wave to be captured by this wavenumber-frequency domain filter, it needs by definition to oscillate regularly in the time dimension, which the Brewer-Dobson circulation does not. Also note that N2 anomalies associated with accelerations of the BD circulation (during polar vortex disturbances) in Fig. 7b are clearly present even after subtracting all the wave anomalies.

2. Structure of temperature anomaly:

The temperature structure shown in Fig. 2 (and discussed in several parts in the manuscript) is more similar to that of gravity waves rather than that of Rossby waves. Although vertically propagating Rossby waves (with wavenumber 1, 2) have westward tilt, the tilting is not big enough to make strong N2 modulation at the tropopause (see Fig.7 of Fletcher and Kushner 2011 for example). Synoptic-scale waves could make strong modulation in temperature and N2 near the tropopause, but their temperature structure is different from that shown in Fig. 2. Based on Hoskins et al. (1985, their Fig. 15), the (potential) temperature and inferred N2 anomalies have horizontally flat structure near the tropopause. It show dense packing of isentropes over high pressure system implying strengthening of the TIL over anticyclones (this feature is constant with the idea of vertical convergence). If authors think that transient waves in 4-25-day frequency band are major contributor and Fig. 2 is their common temperature structure, it should be obtained from observation (not from conceptual figure).

In the new subsection 2.4, we explain the wave modulation mechanism in more detail now. This mechanism applies to waves with any tilt. As long as they are large enough, even wave anomalies with vertical or flat tilt can modulate the tropopause height within a certain longitude range, and therefore have an effect on the tropopause-based seasonal zonal mean profile. Both our filtering method and the wave modulation mechanism are valid for any vertical tilt of the waves. We now see that this wasn't highlighted enough in the previous manuscript.

In the conceptual Fig. 2 we sketch an idealized case to show clearly how the wave modulation mechanism works with the most common extratropical wave type, the upward-propagating Rossby wave. Fig. 3 then shows how this looks like from GPS-RO observations, and particularly Fig. 3c is very similar to the sketch from Fig. 2a which is highlighted in the text. The wavenumber-frequency domain band shown in Fig. 3c is then the dominant one in the seasonal, tropopause-based mean signature of the waves in Figs 4, 6, 8 and A1, which we again link to Rossby waves several times in section 4.

In the new section 5 (Discussion) we link our wave modulation mechanism to earlier literature about cyclone-anticyclone and isentrope packing, among other previously proposed mechanisms.

Regarding the references to Hoskins et al. (1985, their Fig. 15) and the experiments by Fletcher and Kushner (2011):

Axisymmetric vortices are found seldom in the real atmosphere, the closest examples being tropical cyclones or the centers of very strong extratropical cyclones undergoing a warm seclusion. Most often the near-tropopause vertical and horizontal features are far more complex than that. Still, our filtering method does capture wave structures with flat vertical tilt, so in the events where axisymmetric vortices are present, they are included within the filtered signal.

Global climate model experiments where planetary Rossby and synoptic scale waves are studied usually do not have enough vertical resolution to resolve on their own the behavior of these waves near the tropopause. The one by Fletcher and Kushner (2011) for example has 24 vertical levels, which is roughly 1.5km near the tropopause. What we see from GPS-RO observations is that planetary and synoptic-scale waves develop features that have a very short vertical scale, whereas GCMs generally tend to show a too smooth tropopause region (Gettelman et al., 2010; Hegglin et al., 2010). For this reason we are careful not to link our filtered wave signals with model studies about extratropical waves. As stated in subsection 2.3, the purpose of this paper is not to disclose particular properties of the waves, but their overall impact on the TIL (l. 250-254).

## Point-by-point responses to Ref#2

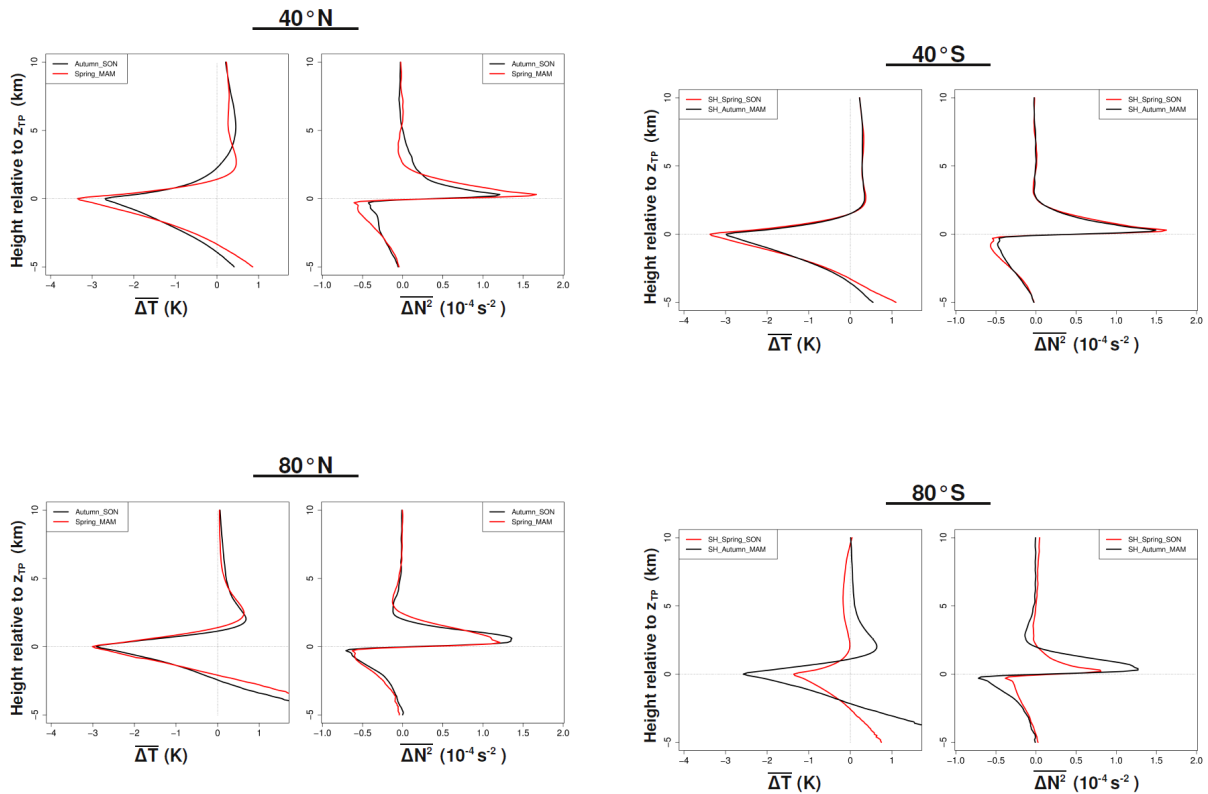
### Major Comments:

Line 278: Regarding Fig. 3: Are the tropopause zonal structures calculated directly from the GPS-RO or from the tropopause-base coordinate? Does it make any difference? Also, if these are zonally averaged tropopause heights, it should state so in the Fig. 3 caption.

The tropopause zonal structures in Fig. 3 are obtained from GPS-RO, which is now stated in the figure caption. Note that in the subsection 2.2, we explain that the tropopause heights are gridded as well, which serves as the base coordinate for averaging later on. No zonal structures in tropopause height are obtained from any zonal average. The zonal means in Figures 4-9, A1 and A2 are averaged with respect to the GPS-RO observed (gridded) tropopause heights.

The paper mentions summer/winter differences in discussing Figs. 5, 7, and 9, yet it appears as if some the largest TIL events occur more in the spring, assuming the year tick marks denote the start of the new year. Would it be useful to discuss the results in terms of four seasons instead of just two?

The stronger TIL in late winter/spring is related to SSWs, but the overall TIL enhancement from extratropical wave modulation is well explained with the winter and summer mean tropopause based anomalies.



We calculated the autumn and spring equivalents of Figs. 4, 6, 8, A1 (e,f). Autumn tends to yield similar results as summer, while spring tends to be close to winter results, except from 80°N where they are intermediate. We mention this now in the corresponding subsections (see lines 423, 482, 582 and 748).

Minor Comments:

Line 2: Probably should be something like “...how much amplitude and variability of the Tropopause Inversion Layer (TIL) comes from modulation by...” (optional)

Corrected. We prefer to use the expression 'strength' instead of 'amplitude' when referring to the TIL.

Line 10: Once again: “The instantaneous modulation...” of the tropopause?, the TIL? I think it would read better if it explicitly states what is being modulated. (optional)

We specify what's modulated by the waves (the temperature field and its gradients around the tropopause) in the first paragraph now, so it applies to the rest of the abstract when we refer to modulation again.

Line 12: “...minor importance for the TIL amplitude and variability...” (optional)

Corrected.

Line 29: “...all latitudes...” The paragraph begins with discussing the extratropical TIL so does “all latitudes” include the tropics too or just extratropics?

Indeed it also includes the tropics. We substituted 'all latitudes' for 'globally'.

Line 120: The paragraph beginning on line 120 starts with ERA-Interim and ends discussing GPS-RO. It seems awkward. Also, this appears to be the only mention of the ERA-Interim winds. It might improve the reading to tell how the ERA-Interim winds will be used to place the GPS-RO observations into a broader context by identifying SSW events and seasonal wind changes. It also might be a good idea to acknowledge the source of the winds explicitly in the appropriate figure captions as well. (optional)

The last paragraph of subsection 2.1 was split into two: the second refers to ERA-Interim exclusively and explains the purpose of the use of reanalysis winds: to show seasonality and polar vortex disturbances, complementing GPS-RO information.

We added ERA-Interim as the source for the winds in the caption of Fig. 5 (this wasn't necessary in the captions of Figs. 7, 9 and A2, since they refer back to Fig. 5 already).

Line 165: “...all...” Weather sometimes changes more rapidly than 2-days. Maybe the “all” should be qualified to “most of” or “the majority of”. (optional)

Corrected (for 'most of').

Line 194: “...and frequency...” “and lower frequency” maybe

Corrected.

Line 333: “...highest period...” maybe “longest period” would read better.

Corrected.

Line 368: “...TIL is clearly discernible in winter...” Maybe eliminate the word “clearly”, as these features are relatively small in Fig. 5. Also, the TIL may be more distinct in spring than in winter (see second major comment).

We now point to “winter and into spring” when referring to when the strongest TIL occurs in Fig. 5a. We would prefer to keep the expression 'clearly discernible': although the TIL is a narrow feature in the vertical dimension, the contrast between the lowermost stratosphere (dark blue color) and the TIL static stability values (orange to red) in winter/spring is striking even at first glance in Fig. 5a, and worth highlighting in our opinion.

Line 529: “...clear TIL during summer months...” Once again, maybe eliminate the work “clear”, and the timing of the maximum TIL may be more toward spring than summer, but it is difficult to tell from the figure.

We now point to “summer and into autumn” when referring to the strongest TIL occurrence in Fig. 9a. We prefer not to take out the word 'clear' for the same reason as in the previous comment.

Other:

Some acronyms/variables are not defined where first introduced. These include: COSMIC GPS-RO (line 5),  $z$  (line 115), TPz (line 117), WMO (line 17), NCL (line 173).

Thank you for pointing this out, we also found the same happening with NH-SH and each acronym is properly defined now.

### **Point-by-point responses to Ref#3**

#### Major comments

1. A key aspect of this whole paper is the recognition that the purely adiabatic impact of a wave on static stability in the tropopause region and the concomitant modification of the tropopause height may lead to a systematic TIL enhancement. Figure 2 serves as a motivation and explanation. However, I did not quite understand the related description in lines 258-260, which seems to present a key argument in this context. Please clarify.

Several times in the text (e.g. bottom of page 9) the authors stress that they typically expect a westward phase tilt with height corresponding to upward propagation of waves. This may be OK for planetary waves, but synoptic-scale waves tend to be evanescent in the stratosphere, so I would not expect much of a phase tilt in the lower stratosphere. In addition, wave modes which represent baroclinic instability (like in the Eady model) do have a westward tilt with altitude regarding perturbation geopotential or the perturbation streamfunction, but the associated tilt of the temperature anomaly actually has an eastward tilt with height (see Fig. 8.10 in the textbook of Holton 2004). Also, it has been argued in the past that some gravity wave activity is actually generated in and,

hence, emanates from the tropopause region (O'Sullivan and Dunkerton, 1995), and the phase tilt of such waves seems less clear or may be insignificant. How does this affect the arguments presented in the paper, which evoke a westward tilt with altitude?

We expanded Figure 2 (new panels 2b and 2c) and the text corresponding to lines 258-260 to better explain the wave modulation mechanism and how it affects the T profile, the local lapse-rate around the tropopause and ultimately tropopause height.

Regarding the wave vertical tilt, both our filtering method and our wave modulation mechanism apply to waves with any possible vertical tilt. We start by showing an idealized example with the commonest wave type (upward-propagating Rossby wave), but now we also explain how this can work with any wave type. We added several paragraphs in subsections 2.3 and 2.4 to clarify this.

Regarding GW and IGW generated near the tropopause: our filtering method is valid for any possible vertical phase tilt of the wave's temperature structure, but since we use a daily dataset it can only filter out waves with periods of 2 days or longer, this excludes IGW and GW that have shorter periods (see last paragraph in section 2.2).

Should GWs and IGWs have an imprint on the zonal-mean, tropopause-based N2 profile and the TIL, this would be visible in Figs. 5b, 7b, 9b, and A2b, but these figures rather point to SSWs events and the polar summer TIL.

2. Fig. 3 shows a few selected cases. Are these random picks, or are these cases where the wave signal at the tropopause level can be seen best. If the latter is true, this would mean that often the wave signal may be rather incoherent and hard to interpret?!

Fig. 3 shows cases where there is a clear modulation of the tropopause zonal structures by the wave anomalies. The picks are thus not random, but nevertheless they weren't difficult to find. During seasons where the wave signature on the TIL is strongest (mid-latitude winter and polar summer), the band corresponding to Fig. 3c shows a clear modulation of the tropopause nearly every day. Then, also almost every day, one or a couple of other bands show significant zonal ranges of tropopause modulation at the same time. We added a short caveat mentioning this in lines 367-372.

Adding to this, the mean wave signatures on the tropopause-based vertical profiles (Figs. 4-9, A1 and A2) further show evidence that the wave modulation is happening systematically.

3. In their interpretation sections, the authors could tie their results more comprehensively to earlier studies, including model studies, in particular the one by Miyazaki et al. (2010), who systematically quantified different mechanisms for TIL formation in a GCM including their hemispheric and seasonal behavior. Also, to what extent does the currently analysis (implicitly or explicitly) include the traveling cyclones and anticyclones which have been argued before to play a role for TIL formation, and to what extent are the current results consistent with the mechanisms suggested earlier? authors choose to leave this as a remaining question (see Page 12), but it could at least be formulated explicitly as a question.

We followed this suggestion. In the new section 5, we link our wave modulation mechanism to isentropic packing above anticyclones (Wirth 2003, 2004), wave breaking (Erler and Wirth 2011) and radiative effects from water vapor / clouds (Miyazaki 2010, Kunkel et al. 2016,

Ferreira et al. 2016). We suggest that our wave modulation mechanism integrates some previously proposed TIL enhancing mechanisms, rather than being a completely different dynamical feature in the tropopause region.

4. I do not like the use of the terms 'warming' and 'cooling'. The authors consider band-with filtered wave signals, in other words anomalies from the zonal mean. If a plot shows a local warm or cold anomaly, this does not necessarily imply that there is/was warming or cooling. It could just as well be the result of horizontal advection, i.e. the original air was replaced by warmer or colder air, but this does not imply any warming or cooling (neither diabatic nor adiabatic). Using more precise terminology would make the discussion of the processes more lucid.

We removed the following sentence from the first paragraph in section 4: “When using the terms cooling/warming, we refer to the net effect of extratropical waves on the tropopause-based zonal mean profile, since certain levels are cooler/warmer in the seasonal mean profile due to these waves. “

... and we substituted the terms warming and cooling for “warm anomaly” and (mean) “cold anomaly” throughout the manuscript.

#### Minor issues

1. Line 86: replace “high amounts of ....” by a more idiomatic expression.

Replaced for “large amounts”.

2. Line 110: the 100 m vertical resolution of GPS-RO temperature profiles, is this really comparable to the vertical resolution of radiosondes? I thought that the latter have even significantly higher resolution. To be sure, I believe that 100 m resolution is sufficient for the purpose of the current paper.

Radiosonde data have higher vertical resolution (several tens of meters), this is true, but GPS-RO with around 100m are not far away; and the theoretical limit of the RO technique, which could be implemented in the future, is of around 40-60m. We rephrased this sentence into “The vertical resolution and height range of the COSMIC GPS-RO temperature profiles are *close to those of* radiosonde data” to avoid any disagreement.

3. Line 126: replace “grid with 10° separation” by a better expression (grid points may have a separation, but not the grid itself).

Replaced for “regular 10° longitude grid”.

4. Line 128: replace 'exponentially-folding function' by 'Gaussian function'

Corrected.

5. Line 153: replace “+- 1 longitude grids” by a better expression (and same with time-discretization)

replaced for “... are filled by averaging neighboring grid points (first +-1 in longitude, then +-1 in time)”.

6. Line 157: replace “in the equator” by “on/at the equator”

Corrected.

7. Line 160: replace “lower bottom of the vertical scale” by “lower bound of the vertical scale”

Corrected.

8. Line 180: replace “remaining of this section” by "remainder of this section"

Corrected.

9. Line 203: this dispersion relation seems to be the version for the shallow water system, right? If so, this should explicitly be stated, and it should also be motivated to what extent this can be used in the current context. After all, the paper deals with the vertically stratified atmosphere, not with the shallow water model. The term “equivalent depth” should then be explained, and also in what sense the term  $f^2/gh$  can be considered as an “approximation to account for vertical propagation”.

Quasi-geostrophic theory is an approximation that uses the shallow water equations, so this is already implied when we refer to the wave as a disturbance propagating in a quasi-geostrophic flow.

We now refer to the  $f^2/gh$  term as “*the vertical wavenumber describing the vertical propagation of the wave in terms of equivalent depth*”.

Regarding the explanation of equivalent depth (the mean depth of the thin layer of fluid on a sphere in the shallow water system of the quasi-geostrophic approximation), we feel that we already describe the used dispersion relation of the Rossby wave in detail. For more, the readers are referred to the book by Andrews et al. (1987).

We feel that a discussion of whether the quasi-geostrophic approximation can be used to describe waves in the stratified atmosphere is not necessary, since it serves only as a simple motivation and is not used in our study at any point. We state several times that our manuscript is focused on the TIL and its enhancing mechanisms, not on particular properties of atmospheric waves.

The use of this idealized approximation to define the Rossby wave is motivated in the two paragraphs that follow: even with this very idealized case, the dispersion relation can be in any place within the wavenumber-frequency domain, depending on the background winds. We now specifically state that taking into account more processes (meridional propagation, horizontal/vertical wind shear), the picture gets even more difficult → thereby the choice of broad filter regions instead of following a specific dispersion curve (which is futile since it would only capture the waves occurring within a certain range of zonal winds!).

10. Bottom of page 7: I find it misleading to talk here about “different wave types”.

As the authors show quite clearly, there is a broad spectrum of waves, which cannot be classified into different types as in the tropics. This is, by the way, exactly what the authors say themselves on page 10 (“unable to differentiate particular wave types”). Maybe one should simply refer to “different parts of the spectrum”.

We followed this suggestion: when we refer to our filtered signals (the different wavenumber-frequency domains defined in Fig. 1, and the resulting filtered anomalies) we replaced “wave type(s)” for “wave spectrum region(s)” throughout the paper.

The references to equatorial waves or specific extratropical waves (e.g. baroclinic Rossby wave) that are not part of our results are kept as “wave types” since they classify as such.

11. Line 236: replace “is outstanding” by a more idiomatic expression.

Replaced for “...their filtered signal stands out from the (unavoidable to filter) background noise”.

12. Line 249: replace “associated to” by “associated with”.

Corrected.

13. Line 267: replace “would remain the same despite the presence of wave anomalies” by “are unaffected by the wave anomalies”

Corrected.

14. The longitude-height sections of Fig. 3 could be improved by actually plotting all the way from  $-180^\circ$  to  $+180^\circ$ .

Our longitude grid goes from  $-175^\circ$  to  $175^\circ$  (with  $10^\circ$  spacing between grid points): there is no zonal grid point missing in Fig. 3 and all the information is within the plots. Unfortunately the plotting function adjusts to the zonal grid and does not interpolate between both ends to close the circle. Note that we cannot use a grid starting at  $-180^\circ$  and ending at  $180^\circ$  for the space-time filtering: both ends are on the same meridian and would lead to errors in the filtered signals because one grid point would be repeated.

15. Line 360: In what sense it  $s = 0$  a wave?

It represents zonally-symmetric, annular oscillations in time (any possible pole-trapped wave mode). We include this now in lines 245-246.

16. Line 511: I would try to avoid the abbreviation “mSSW”.

We substituted this abbreviation for “major SSW” throughout the manuscript.

17. Line 611: replace “humbler” by “smaller”

Corrected.

18. Figure 2: put axes labels, i.e. longitude (or  $\lambda$ ) and altitude (or  $z$ ).

This is surprising to us since Figure 2 in our submitted manuscript (and several previous draft versions that we checked) had both labels, which are somehow missing in the version with the ACPD header. We will contact the Copernicus support team about this issue if still present in the new version.

19. In figure 5 (and all corresponding figures showing time versus altitude) one might consider plotting only up to 30 km, without changing the vertical extent of the plot. This would give somewhat better resolution in the vertical, putting more emphasis on the features around the tropopause region, which is relevant here. On the other hand, the information way up in the stratosphere is not very relevant for this paper (except where discussing stratospheric warmings).

Figs. 7 and 9 show major/minor/final stratospheric warmings, so the proposed change in the vertical scale would affect only Figs. 5 and A2. The visibility of the TIL in all these figures is good already, and we advocate to keep the same format for all Figures 5, 7, 9, and A2 for consistency throughout the paper.

## **Point-by-point responses to interactive comment by A. P. Ferreira**

### Specific comments

Line 4: the phrase “it also puts other TIL enhancing mechanisms into context” should read as “it also puts other TIL enhancing dynamical mechanisms into context”, since radiative effects are not addressed in the study.

It is true that the wave modulation (dynamical) mechanism is investigated in our paper, but when we subtract the wave anomalies (Figs. 5b, 7b, 9b, and A2b) the TIL that remains there can be due to any other mechanism (dynamical or not), including radiative or any diabatic processes, whose overall contribution to the TIL is by extension put into context and discussed throughout section 4 (and also 5 now). Therefore we prefer to keep this sentence as is.

Lines 10-11: instead of “The instantaneous modulation by planetary and synoptic-scale waves is almost entirely responsible for the TIL in mid-latitudes”, it would be more accurate to say: “Planetary and synoptic-scale waves are almost entirely responsible for the instantaneous modulation of the TIL in mid-latitudes”. In this way, the role of radiation is not left out, while keeping the authors’ main finding (wave modulation of the mid-latitude TIL).

We feel that the original sentence in l.10-11 already implies that wave modulation is not totally responsible for the mid-latitude TIL, and prefer to keep it as is. However, we find that your comments about the role of radiation for the mid-latitude and polar TIL are worth addressing in our paper, which we discuss in detail in section 5 now.

Lines 18-20: “After many modelling studies (...) in the last decade, our study finally identifies which processes dominate the extratropical TIL strength and their relative contribution, by analyzing observations only.” The sense of this sentence is questionable because the present and previous works on the extratropical TIL have dealt with different time and/or spatial scales, so they are not easily comparable; besides the FDH sensitivity tests supporting the radiative hypothesis are a mix of observations and radiative modelling. I am sure that the authors do not want to say that the previous theories are all marginal to the subject. Then, it would be more constructive to write something like, “In addition to the TIL enhancing mechanisms proposed by modeling studies in the last decade, our study now identifies which dynamical processes dominate the zonal-mean extratropical TIL strength and their relative contribution, by analyzing observations only.”

This is a fair point, perhaps this paragraph came out too strong. We rephrased the beginning of the paragraph containing l.18-20 to make it more inclusive.

Our point of view is that our wave modulation mechanism rather integrates several previously proposed mechanisms: particularly radiative effects from water vapor and clouds, and the isentrope packing above anticyclones (e.g. Wirth 2003, 2004), they should be included in the filtered wave signal since they travel with the wave and its embedded cyclones-anticyclones. We discuss this in detail within the new section 5.

Lines 363-364: it would be helpful to the reader to clarify the expression “TIL enhancement” (from the values given in the text, it refers to the increase of  $N^2_{max}$ ). Since it is used more than once, it should be explained in the introductory part of section 4.

We added a specification in the first paragraph of section 4.1 linking the  $N_2$  increase above the tropopause to the TIL enhancement.

Lines 380-381: when saying that the TIL is “almost completely gone” after subtracting the extratropical wave signal, the authors meant to say that  $N^2_{max}$  is greatly reduced. This might be clarified in parenthesis.

We feel that an additional clarification after this sentence is not necessary: the reduction in  $N_2$  is specified in detail right after this sentence in the remainder of the paragraph.

Lines 501-502: “The only other mechanism restricted to polar summer that could enhance the TIL is water vapor radiative cooling of the tropopause”. The word “restrictive” seems misleading here. I would suggest rephrasing in this way: “The only other mechanism that could enhance the polar summer TIL is water vapor radiative cooling of the tropopause”.

We rephrased this sentence into: “The only other known mechanism that could enhance the TIL in polar summer is water vapor radiative cooling of the tropopause”. We also made the same change in the Concluding Remarks (sec. 6) in a phrase which used a similar expression.

Lines 559-560: Since the text refers specifically to “the remaining TIL”, I would suggest to replace “is enhanced by” → “is due to”

We followed this suggestion.

Figures 5, 7, 9: in Figure 5, we expected to see  $N^2$  values in the range  $1-2 \times 10^{-4} s^{-2}$  in the upper troposphere. So, I don't understand why  $N^2$  is shown in white (or is not shown) below the tropopause. The same applies to Figures 7 and 9, even if the high-latitude upper-troposphere static-stability values are different. I guess this was done to enhance the color map in the lower stratosphere. Anyhow, values not shown in the plots should be mentioned at some point (e.g., figure caption of Figure 5).

We added a specification in Fig. 5 caption that tropospheric  $N_2$  values are left blank. Figs. 7, 9, and A2 later refer back to Fig. 5.

## **References:**

Gettelman et al. (2010), Multi model assessment of the upper troposphere and lower stratosphere: Tropics and global trends, *Journal of Geophysical Research (Atmospheres)* , 115 , D00M08, doi: 10.1029/2009JD013638.

Hegglin et al. (2010), Multimodel assessment of the upper troposphere and lower stratosphere: Extratropics, *Journal of Geophysical Research (Atmospheres)* , 115 , D00M09, doi:10.1029/2010JD013884.

Wheeler, M. and Kiladis, G. N. (1999) Convectively Coupled Equatorial Waves: Analysis of Clouds and Temperature in the Wavenumber-Frequency Domain., *Journal of Atmospheric Sciences*, 56, 374–399, doi:10.1175/1520-0469(1999)056<0374:CCEWAO>2.0.CO;2

# Wave Modulation of the Extratropical Tropopause Inversion Layer

Robin Pilch Kedzierski<sup>1</sup>, Katja Matthes<sup>1,2</sup>, and Karl Bumke<sup>1</sup>

<sup>1</sup>Marine Meteorology Department, GEOMAR Helmholtz Centre for Ocean Research Kiel, Kiel, Germany.

<sup>2</sup>Faculty of Mathematics and Natural Sciences, Christian-Albrechts-Universität zu Kiel, Kiel, Germany.

*Correspondence to:* Robin Pilch Kedzierski (rpilch@geomar.de)

## Abstract.

This study aims to quantify how much of the **observed strength and variability of the zonal-mean extratropical Tropopause Inversion Layer (TIL) comes from the modulation of the temperature field and its gradients around the tropopause** by planetary and synoptic-scale waves. By analyzing high-resolution observations, it also puts other TIL enhancing mechanisms into context.

Using gridded **Global Positioning System radio occultation (GPS-RO) temperature profiles from the COSMIC mission (2007-2013)**, we are able to extract the extratropical wave signal by a simplified wavenumber-frequency domain filtering method, and to quantify the resulting TIL enhancement. By subtracting the extratropical wave signal, we show how much of the TIL is associated with other processes, at mid and high latitudes, for both Hemispheres and all seasons.

The instantaneous modulation by planetary and synoptic-scale waves is almost entirely responsible for the TIL in mid-latitudes. This means that wave-mean flow interactions, inertia-gravity waves or the residual circulation are of minor importance **for the strength and variability of the mid-latitude TIL.**

At polar regions, the extratropical wave modulation is dominant for the TIL strength as well, but there is also a clear fingerprint from sudden stratospheric warmings (SSWs) and final warmings in both hemispheres. Therefore, polar vortex breakups are partially responsible for the observed polar TIL strength in winter (if SSWs occur) and spring. Also, part of the polar summer TIL strength cannot be explained by extratropical wave modulation.

**We suggest that our wave modulation mechanism integrates several TIL enhancing mechanisms proposed in previous literature while robustly disclosing the overall outcome of the different processes involved. Our study identifies which mechanisms dominate the extratropical TIL strength and their relative contribution, by analyzing observations only.** It remains to be determined, however, which roles the different planetary and synoptic-scale wave types play within the total extratropical wave modulation of the TIL; and what causes the observed amplification of extratropical waves near the tropopause.

## 1 Introduction

The extratropical Tropopause Inversion Layer (TIL) is a strong temperature inversion at the extratropical tropopause with a corresponding static stability maximum right above. It is a fine-scale feature discovered via tropopause-based averaging (Birner et al., 2002; Birner, 2006), consisting of a thin layer of about 1km depth. Satellite Global Positioning System radio occultation observations (GPS-RO) show that the TIL is present globally (Grise et al., 2010).

The TIL is established as an important feature of the extratropical upper troposphere and lower stratosphere (UTLS) (Gettelman et al., 2011), and it is of interest to the scientific community for the following reasons: high static stability values theoretically affect the dispersion relations of atmospheric waves like Rossby or Inertia-Gravity waves since this parameter is part of different wave theory approximations (see Birner (2006); Grise et al. (2010) and references therein). In an idealized model experiment, Sjoberg and Birner (2014) showed that the TIL acts as a partial barrier for upward wave propagation. The study by Zhang et al. (2015) supports this hypothesis by showing inhibited upward propagation of Inertia-Gravity waves (IGW) due to the TIL, with data from a single US radiosonde station. Also, the TIL is likely to inhibit the cross-tropopause exchange of chemical compounds: high static stability suppresses vertical motion and is correlated with strong trace gas gradients (Hegglin et al., 2009; Kunz et al., 2009; Schmidt et al., 2010). In the next paragraphs we shortly review what is known so far about the observed variability of the extratropical TIL and the mechanisms proposed for its formation/enhancement.

Climatological studies about the seasonal, zonal-mean state of the TIL show that it reaches maximum strength during polar summer while it displays a weaker relative maximum in winter mid-latitudes (Birner, 2006; Randel et al., 2007; Randel and Wu, 2010; Grise et al., 2010). From a synoptic-scale perspective, the TIL in mid-latitude winter has very pronounced zonal structures, and the TIL within ridges (anticyclones) in mid-latitude winter has the same strength or even higher than any TIL observed in polar summer (Pilch Kedzierski et al., 2015). The cyclone-anticyclone modulation with weaker-stronger TIL is found at all extratropical latitudes and seasons (Randel et al., 2007; Randel and Wu, 2010; Pilch Kedzierski et al., 2015).

Different mechanisms are responsible for the formation/maintenance of the extratropical TIL:

- Radiative cooling below the tropopause by water vapor due to its strong gradient across the tropopause acts to enhance the TIL (Randel et al., 2007; Hegglin et al., 2009; Kunz et al., 2009; Randel and Wu, 2010), and a high-resolution model study by Miyazaki et al. (2010b, a) showed that radiative effects are dominant in polar summer, while dynamics enhance the TIL otherwise. Other modelling studies suggest that radiation and diabatic processes related to water vapor and clouds could share importance with dynamics in strengthening the mid-latitude TIL (Ferreira et al., 2016; Kunkel et al., 2016).

- The downwelling branch of the stratospheric residual circulation was proposed to cause dynamical heating above the tropopause and TIL enhancement in a model experiment by Birner (2010).

The first evidence of this was found by Wargan and Coy (2016) at high latitudes following major  
65 sudden stratospheric warmings (SSWs), mainly caused by the convergence of the vertical compo-  
nent of the residual circulation ( $\overline{w^*}$ ). During a major SSW there is an acceleration of the residual  
circulation, and the enhanced  $\overline{w^*}$  convergence is the reason of the downward-propagating positive  
temperature anomaly (Andrews et al., 1987), which in turn enhances the high-latitude TIL once the  
signal reaches the lowermost stratosphere in winter or spring.

70 - Baroclinic waves and their embedded cyclones-anticyclones can enhance the TIL by tropopause  
lifting and cooling, and also warming above the tropopause in anticyclones from vertical wind con-  
vergence (from model experiments by Wirth (2003, 2004); Wirth and Szabo (2007); Son and Polvani  
(2007)). These synoptic-scale dynamics partly explain the seasonality and latitude-dependence of  
the extratropical TIL strength. Also, the baroclinic life-cycle experiment by Erler and Wirth (2011)  
75 showed the importance of baroclinic wave breaking events in enhancing the TIL. However, so far  
there is only observational evidence of the role of synoptic-scale dynamics in the cyclone-anticyclone  
modulation of the (weaker-stronger) TIL (Randel et al., 2007; Randel and Wu, 2010; Pilch Kedzier-  
ski et al., 2015).

- And finally, small-scale inertia-gravity waves (IGW) also play a role in enhancing the TIL.  
80 Kunkel et al. (2014) showed transient TIL modulation and enhancement from the presence of IGW's  
in a baroclinic life-cycle experiment, and proposed that this could persistently enhance/maintain the  
TIL via wave-mean flow interaction. This was confirmed in the study by Zhang et al. (2015), who  
showed that the strong wind shear found within the TIL lead to IGW breaking, downward heat flux  
and tropopause cooling (from a single US high-resolution radiosonde station).

85 The goal of our study is two-fold: 1) quantify how much of the TIL strength in the extratropics  
comes from its modulation by planetary to synoptic-scale waves, and 2) by subtracting the wave  
signal, to identify other processes that enhance the TIL and thereby make an observational confir-  
mation of their relative contribution. Only modelling studies have looked at these processes thus  
far (reanalysis in the case of a major SSW in Wargan and Coy (2016)), or their observation is very  
90 sparse (one single US high-resolution radiosonde station in the IGW study by Zhang et al. (2015)).  
Therefore it is of interest to put the roles of the different TIL enhancing processes, as enumerated  
above, into context by using large amounts of high-resolution global GPS-RO observations from the  
COSMIC mission (Anthes et al., 2008), which is the primary source of high-resolution observations  
of the temperature structure near the tropopause. It has to be pointed out that our focus is oriented on  
95 knowing the total signal of the extratropical (planetary to synoptic-scale) waves, rather than separ-  
ating every possible wave type at each given time, which is not possible in practice given the highly  
variable background wind regimes in the extratropics (see section 2 for more details).

We extract the extratropical wave signal by wavenumber-frequency domain filtering of gridded  
GPS-RO data. Our method is similar to that of Pilch Kedzierski et al. (2016), who quantified the role  
100 of the different equatorial wave types in modulating and enhancing the tropical TIL. Compared to

the equatorial wave filtering, the method in this study is adapted and simplified to account for the distinct wave spectrum and the highly varying wind regimes that are found in the extratropics. We explain how this is done, justifying the filter settings and disclosing the wave modulation mechanism in detail, in section 2; and we provide a proof of concept in section 3, showing that our method is successful in representing the extratropical waves and their TIL modulation. In section 4 we quantify the average signal of the extratropical waves as well as the remaining TIL with this signal removed, for all seasons in the mid- and high-latitudes of the Northern and Southern Hemispheres (NH and SH). We discuss our results and relate the wave modulation mechanism to previous studies in section 5. The main findings are summarized in section 6.

## 2 Data and Methods

### 2.1 Datasets

We analyze GPS-RO temperature profiles measured by the COSMIC satellite mission (Anthes et al., 2008). The effective physical resolution of GPS-RO retrievals is normally  $\sim 1\text{km}$ , improving towards the order of 100m in regions where the stratification of the atmosphere changes, such as the tropopause and the top of the boundary layer, where high vertical resolution is most needed (Kursinski et al., 1997). The COSMIC dataset is provided (interpolated) on a regular vertical grid with 100m spacing, from the surface up to 40km altitude. The vertical resolution and height range of the COSMIC GPS-RO temperature profiles are close to those of radiosonde data, but with the advantages of global coverage, high sampling density of  $\sim 2000$  profiles/day, and weather-independence. Also, the accuracy of GPS-RO profiles is even higher than that of radiosondes (Anthes et al., 2008; WMO, 1996). With the temperature profiles, vertical profiles of static stability are calculated as the Brunt-Väisälä frequency squared ( $N^2 [s^{-2}]$ ):

$$N^2 = (g/\Theta) \cdot (\partial\Theta/\partial z)$$

where  $g$  is the gravitational acceleration,  $\Theta$  the potential temperature,  $z$  the vertical dimension and  $\partial$  its partial derivative. The tropopause height ( $TP_z$ ) was calculated using the World Meteorological Organization lapse-rate tropopause criterion (WMO, 1957). Profiles with unphysical temperatures or  $N^2$  values (temperature  $< -150^\circ\text{C}$ ,  $> 150^\circ\text{C}$  or  $N^2 > 100 \times 10^{-4} s^{-2}$ ) or those where the tropopause was not found were excluded ( $< 1\%$ ).

To extract the extratropical wave signal from the GPS-RO dataset, we first grid the profiles (see subsection 2.2) and then apply wavenumber-frequency domain filters which require data on a regular longitude-time spacing (see subsection 2.3).

To complement the GPS-RO observations, we also use daily-mean vertical profiles of zonal winds from the ERA-Interim reanalysis (Dee et al., 2011) for the years 2007-2013, which provide information about seasonal wind changes or polar vortex disturbances.

## 135 2.2 Gridding of GPS-RO profiles

The COSMIC GPS-RO temperature profiles at certain latitude bands are gridded daily, between 2007-2013, on a regular 10° longitude grid. The latitude bands chosen for this study are 40°N and 40°S to represent the mid-latitudes, and 80°N and 80°S for polar latitudes. These latitude bands were selected because they show the seasonal cycle of the tropopause and TIL best for mid and 140 high latitudes. Throughout section 4, results for the latitudes 40° and 80° will be disclosed for both Hemispheres. The same analyses were performed for the latitude bands in between, 50°-60°-70°, which have an intermediate behavior in each case.

At each grid point, the profiles of that day within +5° latitude and +5° longitude are selected to calculate a tropopause-based weighted average temperature profile and the corresponding  $N^2$  145 vertical profile:

$$T_{grid}(\lambda, Z_{TP}, t) = \sum_i w_i T_i(\lambda, Z_{TP}, t) / \sum_i w_i$$

$$N_{grid}^2(\lambda, Z_{TP}, t) = \sum_i w_i N_i^2(\lambda, Z_{TP}, t) / \sum_i w_i$$

where  $\lambda$  is longitude,  $Z_{TP}$  is the height relative to the tropopause and  $t$  is time. The weight  $w_i$  is a Gaussian function that depends on the distance of the GPS-RO profile from the grid center, taking 150 longitude, latitude and time (distance from 12UTC):

$w_i = \exp(-[(D_x/5)^2 + (D_y/5)^2 + (D_t/12)^2])$ , where  $D$  are the distances in °longitude (x subscript), °latitude (y) and hours (t). The maximum distance allowed from the grid point in each dimension is: 5° longitude, 5° latitude, and 12 hours from 12UTC, respectively.

The gridded tropopause height ( $\lambda, t$ ) is calculated with the same weighting of all profiles' tropopauses. 155 The gridded temperature and  $N^2$  profiles are shifted, as the last step, from the tropopause-based vertical scale onto a ground-based vertical scale from 5km to 35km altitude, obtaining a longitude-height array for each day of 2007-2013.

Most often 2-3 profiles are selected for averaging at a grid point with these settings, although one GPS-RO profile is sufficient to estimate a grid point. However, in 14.8% of the cases the algorithm 160 does not find any profile. To fill in the gaps, the longitude range to select the profiles is incremented to +10° instead of +5°, and the latitude range is also incremented to +7.5° instead of +5°, which then leaves a 1.8% of empty grid-points. For this minority, profiles are selected within +-1day and +-15° longitude (and same latitude settings). In all cases the weighting function remains the same. The

remaining data gaps (0.06%) are filled by averaging neighboring grid points (first +-1 in longitude, then +-1 in time). These exceptions are for a very small portion of the gridded data, and therefore do not affect the retrieved wave signatures after filtering (the percentages showed in this paragraph are for the Northern Hemisphere, and they are similar in the SH).

This gridding method is very similar to the one used by Pilch Kedzierski et al. (2016) at the equator, developed after Randel and Wu (2005). The higher GPS-RO density in the extratropics allowed for a narrower latitude range to select profiles around a latitude band in order to minimize meridional smoothing of the extratropical TIL properties. The lower bound of the vertical scale is set to 5km to account for the lower extratropical tropopause heights compared to the equator.

Once gridded, for each latitude band, we end up with a daily longitude-time array of temperature and  $N^2$  for each level between 5-35km with 100m vertical spacing. With a daily temporal resolution, this dataset resolves waves with periods of 2 days or longer, or frequencies of 0.5 cycles per day (cpd) or lower, which is enough to capture most of the planetary and synoptic-scale extratropical waves. Note that the inertial frequency in the extratropics ranges from  $\sim 1.3$ cpd at  $40^\circ$  latitude to 2cpd at the poles, so inertia-gravity waves (IGW), with frequencies between the inertial and the much higher buoyancy frequency, cannot be resolved with these settings (Andrews et al., 1987). However, by extracting the combined planetary and synoptic-scale wave signal and subtracting it later, we can indirectly infer how important is the role of IGWs or other processes in enhancing the extratropical TIL.

### 2.3 Wavenumber-Frequency Domain Filtering

With the longitude-height-time array of gridded temperature and  $N^2$  profiles obtained in the previous subsection 2.2, we make use of the freely available 'kf-filter' NCAR Command Language (NCL) function (Schreck, 2009) to filter in the wavenumber-frequency domain. For each vertical level (from 5km to 35km height with 100m vertical spacing), we retrieve a longitude-time array which is detrended, tapered in time and space-time bandpass filtered with a two-dimensional Fast Fourier Transform. This methodology is analogous to that of Pilch Kedzierski et al. (2016), who filtered gridded equatorial GPS-RO data in certain regions of the wavenumber-frequency domain, following the dispersion curves of the different equatorial wave types which have clear spectral signatures in those wavenumber-frequency domains (Wheeler and Kiladis, 1999). In the remainder of this subsection we will explain how the filter bounds in the wavenumber-frequency domain were chosen in this study to adapt the method of Pilch Kedzierski et al. (2016) to the extratropics.

The extratropical wave modes differ greatly from those at the equator: they are not equatorially trapped and can propagate in any direction, the Coriolis parameter has to be taken into account, and the zonal wind regimes in the extratropics are much more variable than the equatorial ones. At sub-seasonal time-scales, the Northern Annular Mode (NAM) can alter the strength of the prevailing westerlies in the extratropical troposphere and lowermost stratosphere; there is a strong seasonal

200 cycle in the stratosphere with very strong westerlies (several tens of m/s) within the winter polar vortex, changing to easterlies (-10 to -20 m/s) in summer; and the polar vortex is disrupted very quickly during major SSWs. These modes of variability of the zonal winds in the extratropics have higher amplitude and frequency than any wind regime shifts found at the equator, which has a relatively weak seasonal cycle, and the quasi-biennial oscillation (QBO) in the stratosphere still has less  
 205 amplitude and lower frequency compared to the polar winter vortex - summer anticyclone. Background winds affect the propagation of waves, by doppler-shifting their dispersion relations or even precluding their propagation, therefore it is of special importance to take them into account in the extratropics.

We make a comparison of the dispersion curves of the extratropical Rossby wave under different  
 210 background zonal wind regimes in Figure 1. The Rossby wave dispersion relation is defined as the most common form of large-scale wave disturbance found in the extratropics: a planetary wave forced from the troposphere, and propagating vertically and zonally in a quasi-geostrophic flow. Assuming  $N^2$  and background mean zonal winds ( $\bar{U}$ ) to be constant, and no meridional propagation for simplicity, the following dispersion relation can be obtained (following Andrews et al. (1987)):

215 
$$w = s\bar{U} - s\beta[s^2 + f^2/gh]^{-1}$$

where  $w$  is the frequency,  $s$  is the zonal wavenumber,  $f$  the Coriolis parameter,  $\beta$  its meridional derivative at a certain latitude (the Beta-plane approximation),  $g$  the gravity acceleration and  $h$  the equivalent depth. Since we assume no meridional propagation for simplicity, the meridional wavenumber is set to zero so it is absent in this formula (compared to Andrews et al. (1987)). The  
 220 term ( $s\bar{U}$ ) accounts for the doppler-shifting of the dispersion relation by the background zonal winds; and the ( $f^2/gh$ ) term is the vertical wavenumber describing the vertical propagation of the wave in terms of equivalent depth.

In Figure 1, we show how the dispersion curve of a Rossby wave changes depending on its equivalent depth (different line types), and the background zonal mean winds (zero winds black, blue  
 225 for easterlies, red for westerlies, see specific arrows outside the diagram). Note that each dispersion curve is not valid for the entire year for the Rossby wave. For example, a Rossby wave in winter would propagate following the red (10m/s) dispersion relation in the lowermost stratosphere (i.e. the bottom of the polar vortex); at higher levels (the core of the polar vortex) stronger westerlies are found and the same Rossby wave would propagate following the red (40m/s) curve. At some point  
 230 in spring and autumn, the black curve ( $\bar{U} = 0$  m/s) is theoretically valid, and so is the blue curve (-10m/s) in summer, with easterlies throughout the stratosphere.

The dispersion relations in Fig. 1 show the difficulty of defining a wave type in the extratropics: the dispersion curve for a given wave type (idealized Rossby wave in this case) can be in basically every possible place within the wavenumber-frequency domain, depending on the background winds. In  
 235 reality, there is more complexity when meridional propagation and vertical/horizontal wind shear

are taken into account for the wave's dispersion relation, which would further increase the difficulty of defining it in a certain region of the wavenumber-frequency domain. Therefore, it is impossible to define one filter to extract Rossby waves that is valid for the entire time period (2007-2013) and that could be used at all levels between 5 and 35km altitude.

240 We overcome this difficulty by simplifying the method of Pilch Kedzierski et al. (2016). Instead of defining certain dispersion curves, we use wide boxes in the wavenumber-frequency domain, only differentiating eastward-westward propagating oscillations with respect to the ground and their periods (faster 2-4 day waves; slower 4-25 day waves; and 30-96 day or quasi-stationary waves), which are displayed as the six grey boxes in Fig. 1. We also define a seventh filter for wavenumber  
245 zero ( $s = 0$ , brown box in the middle of the diagram in Fig. 1) for completeness, which represents zonally-symmetric, annular oscillations in time (any possible pole-trapped wave mode). This way, the Rossby waves will be captured by one or another filter, independently of the background zonal winds -together with any other extratropical wave mode that oscillates in those wavenumber-frequency domains. We stress that our gridded data set resolves waves of periods of 2 days or longer,  
250 which excludes IGWs and GWs (see subsection 2.2).

With this method we prioritize knowing the total effect of planetary and synoptic-scale extratropical waves on the TIL, at the cost of not differentiating baroclinic, barotropic, standing, travelling (etcetera) wave modes. We find this to be a fair compromise, since our study targets TIL modulation and enhancement by extratropical waves (successfully, see sections 3 and 4), and not to disclose  
255 particular properties of these waves.

If waves are present, their filtered signal stands out from the (unavoidable to filter) background noise, which appears as a continuum of low-amplitude fluctuations (Wheeler and Kiladis, 1999), and the instantaneous modulation of the tropopause and the TIL by these waves will be captured since these oscillations are resolved by the gridded dataset (see subsection 2.2). When waves are not  
260 present, only the low-amplitude background noise will appear in the filtered signal, and the observed tropopause heights will not be modulated by a non-existing anomaly, therefore having no effect on the tropopause-based means. In this case, the use of broad boxes in the wavenumber-frequency domain for filtering is not a drawback.

The wave modulation mechanism is explained in detail in the next subsection 2.4.

## 265 2.4 The Wave Modulation Mechanism

As mentioned in the previous subsection 2.3, the extratropical wave anomalies are filtered from a longitude-time array: each vertical level of the gridded GPS-RO profiles is filtered independently, and then stored together in a longitude-height-time array of wave anomalies. Therefore, for a given latitude band, we end up with arrays of gridded GPS-RO profiles (temperature and  $N^2$ ), and the  
270 corresponding anomalies (also of temperature and  $N^2$ ) from the seven wave filter bounds defined in Fig. 1, all gridded with  $10^\circ$  longitude, 100m height and 1-day spacing.

When one specific day is selected from these arrays, a longitude-height snapshot of the wave anomalies is obtained. Extratropical waves have vertical tilts in their temperature structures, and if the anomalies are large, they can effectively modulate tropopause height as explained next.

275 Figure 2a shows idealized temperature anomalies associated with an atmospheric wave with westward vertical tilt, as a longitude-height snapshot of the positive/negative (red/blue dashed contours) temperature anomaly structures. The anomalies sketched in Fig. 2a would correspond to that of an upward-propagating Rossby wave (Andrews et al., 1987) which is present around the extratropical tropopause. Any tropospheric or stratospheric anomalies are omitted for simplicity in Fig. 2a, since  
280 they are irrelevant for the instantaneous modulation of the TIL. The local temperature profile would be the result of superimposing the local anomalies to the ground-based zonal mean temperature profile, as depicted in Figs. 2b and 2c.

The thermal tropopause is defined as the point where the lapse-rate changes from typical tropospheric values ( $\sim 7\text{K/km}$  colder with height) to less than  $2\text{K/km}$  for more than  $2\text{km}$  (WMO, 1957).  
285 Therefore, if the wave temperature anomalies are large enough, they could effectively change the point where this criterion is met by deviating the local lapse-rate near the tropopause from that of the zonal-mean profile. Fig. 2b shows a case where the tropopause is lowered due to the wave anomalies, and Fig. 2c another where the tropopause is lifted. The tropopause would tend to be placed above negative stratification anomalies, and/or below positive stratification anomalies, which is most often  
290 centered at the strongest negative temperature anomaly as in both idealized cases in Figs. 2b and 2c.

As explained in subsection 2.3, these temperature anomalies are not only deviations from the ground-based zonal mean profile, but they are also part of a space-time harmonic: they need to be wave-like and to travel in the wavenumber-frequency domain by definition. Local anomalies present in the gridded GPS-RO temperature profiles that are not part of a planetary or synoptic-scale wave  
295 (but the result of other processes) are thus not filtered out.

Note that the tropopause modulation by atmospheric waves sketched in Fig. 2 is highly idealized: usually waves with different wavenumbers, frequencies and vertical tilts can be present simultaneously, making the actual observed tropopause modulation more complex than in Fig. 2. As explained next, our filtering method applies to any vertical tilt.

300 We highlight that the wavenumber-frequency domain filters are applied to longitude-time arrays from each vertical level independently (see subsection 2.3): no filtering is done in the vertical direction. Therefore, if an atmospheric wave is present, it will be captured by our filters regardless of its vertical tilt, as long as at a given level it can be represented by a space(longitude)-time harmonic. The vertical tilt of the wave appears when the filtered anomalies of each vertical level are piled together  
305 (see section 3 and Figure 3).

In Fig. 2 we presented idealized upward-propagating Rossby wave temperature anomalies to sketch the wave modulation mechanism at the tropopause region because this wave type is the commonest in the extratropics. As our filtering method, the wave modulation mechanism also applies

to waves with any vertical tilt. One may just mirror Fig. 2a in the longitude direction to get the  
310 wave modulation by a wave with eastward vertical tilt (e.g. a downward-propagating Rossby wave).  
For waves whose vertical tilt is flat (axisymmetric vortices) or vertical (barotropic wave modes), the  
anomalies do not form a dipole in the vertical direction, but they do so in the longitude direction:  
one may take just the upper (or the bottom) pair of anomalies from Fig. 2b and 2c, and still modulate  
tropopause height from these wave anomalies within a certain longitude range.

315 A tropopause-based mean of the anomalies sketched in Fig. 2a would yield a dipole of cold anomalies centered at the tropopause, warm anomalies above, and a net TIL enhancement just from the presence of the wave in the tropopause region. Note that the ground-based zonal average temperature profile and the zonal mean tropopause height are unaffected by the wave anomalies in Fig. 2a: only the tropopause-based zonal mean profile is affected. To leave an imprint in the tropopause-  
320 based mean, the wave modulation mechanism does not need to be present over the whole longitude range, but only a significant part of it. Sections 3 and 4 will show that this happens constantly due to the near-ubiquitous presence of waves (of any type) near the tropopause region.

We expect that our filtered wave anomalies will modulate the tropopause in a similar fashion as sketched in Fig. 2a for temperature. Once a wave is away from the tropopause region or dissipated,  
325 no filtered signal will affect the TIL, therefore permanent effects from wave-mean flow interaction (wave dissipation or breaking) are not quantified by our method.

Next in section 3, we show examples of the filtered signals and the tropopause adjustment to the extratropical waves, in order to proof the validity of our method to study the extratropical TIL wave modulation.

### 330 3 Proof of Concept

Figure 3 shows snapshots of the longitude-height  $N^2$  anomalies (colors) filtered in the wavenumber-frequency domains defined in Fig. 1 (see previous subsection 2.3), together with the tropopause height (black line), for the 50°N latitude band. Each snapshot is selected for a different winter date, in order to portray cases when there is a clear modulation of the tropopause's zonal structures from  
335 the extratropical wave anomalies. We do not include the  $s=0$  filter since it lacks zonal structures by definition. In Fig. 3 the eastward and westward propagation refers to the movement of the wave relative to the ground as defined in subsection 2.3.

In Fig. 3 there are several analogies to the tropopause and TIL modulation by equatorial waves described in the study by Pilch Kedzierski et al. (2016). In our extratropical case, we also show  
340 tropopause modulation by the wave anomalies when their amplitude is large, with predominant positive  $N^2$  anomalies above the tropopause, and negative  $N^2$  anomalies below, which correspond to the temperature anomalies that modulate tropopause height as sketched in Fig. 2. The modulation by extratropical waves is especially clear in Fig. 3c for eastward-propagating waves with periods of

4-25 days: strong positive  $N^2$  anomalies are detected right above the tropopause between  $-180^\circ\text{E}$  and  $-25^\circ\text{E}$ , while negative  $N^2$  are located below the tropopause between  $25^\circ\text{E}$  and  $180^\circ\text{E}$ . Similarly, in Fig. 3d (westward-propagating 4-to-25-day waves) tropopause height follows the positive  $N^2$  anomalies between  $-75^\circ\text{E}$  and  $180^\circ\text{E}$ . Sometimes positive  $N^2$  anomalies can be located below the tropopause and viceversa, as in the cases shown in Fig. 3 a, b, e and f; but the zonal mean is still dominated by positive  $N^2$  anomalies right above the tropopause. Note that different wave types can be present simultaneously within a single spectrum region defined in Fig. 1, and thus shape together the  $N^2$  anomalies and the tropopause zonal structures appearing in the snapshots in Fig. 3.

It can also be observed in all cases in Fig. 3 that there is a relative maximum of wave activity around the tropopause regardless of the amount of wave activity in the stratosphere, as measured by  $N^2$  anomalies. This is in line with the findings of Pilch Kedzierski et al. (2016) who reported wave amplification near the tropopause for every equatorial wave type.

The westward tilt of the Rossby waves can be discernible in many cases (Fig. 3 a-d) throughout the stratosphere: most clearly in the intermediate periods of 4-25 days which are the most common for travelling Rossby waves, but also visible sometimes in the 30-96 day periods, indicating the presence of quasi-stationary Rossby waves. This is a good indicator that these waves are properly captured by our filters, which are used at each vertical level independently: the vertical structure of the waves is obtained without filtering in the vertical direction. Note that in Fig. 3, planetary and synoptic-scale waves are all superimposed, so the overall appearance is increasingly patchy when short and fast waves are present, which is why Fig. 3 e and f show these structures the most.

The wavenumber-frequency domain filtering method used for extratropical waves (see subsection 2.3 and Fig. 1), although simplified compared to Pilch Kedzierski et al. (2016) and unable to differentiate particular wave types, is able to capture the overall planetary and synoptic-scale extratropical wave signal and how it modulates the tropopause and the TIL as shown in Fig. 3. Although Fig. 3 shows very clear cases for each filtered band, in the seasons where the wave signature on the TIL is strongest (mid-latitude winter and polar summer, see section 4) the modulation of the tropopause height zonal structures by the wave anomalies can be as evident almost every day for the band corresponding to Fig. 3c, with one or more other bands also showing significant zonal ranges of tropopause modulation at the same time.

The examples shown in Fig. 3 are for the  $50^\circ\text{N}$  latitude band in winter, but similar conclusions can be drawn from any extratropical latitude or season. The tropopause-based, seasonal mean of the extratropical wave signal will show an overall TIL enhancement, which is quantified next in section 4 for mid and high latitudes, winter and summer, Northern and Southern Hemisphere.

#### 4 Wave Modulation of the Extratropical Tropopause Inversion Layer

Figure 3 in section 3 showed the tropopause adjustment to the horizontal and vertical structure of the filtered extratropical wave anomalies, with positive  $N^2$  anomalies generally placed above the tropopause, and negative  $N^2$  anomalies below. Therefore, a tropopause-based average of the wave signals should give a net TIL enhancement. We perform the same analysis with the filtered temperature anomalies, which we expect to show a net cold anomaly at the tropopause and a warm anomaly aloft (the dipole needed to enhance  $N^2$  right above the tropopause).

Also, by subtracting the extratropical wave signal from the gridded GPS-RO data, it is possible to show the remaining TIL that is caused by mechanisms other than the extratropical wave modulation. We will present the daily evolution of the vertical tropopause-based  $N^2$  profile, comparing the observed  $N^2$  vertical structure to the one without the extratropical wave signal, which should show a weaker TIL.

Note that the wavenumber-frequency domain filters are not able to extract the wave anomalies at the beginning and end of the 2007-2013 time-period of our study. The longest period filtered is 96 days (see section 2, Fig. 1), therefore data from the first 100 days of 2007 and the last 100 days of 2013 are not used for any figures of this section, in order to make sure that there is no signal missing.

Throughout this section, we will present the two kinds of analysis explained in the previous paragraphs: seasonal, tropopause-based averages of the extratropical wave temperature and  $N^2$  signals; and the time evolution of observed  $N^2$  zonal-mean profiles, with and without the daily extratropical wave signal. Both analyses will be presented for mid-latitudes (40°N, subsection 4.1) and polar latitudes (80°N, subsection 4.2), first in the Northern Hemisphere, and then the exact same methodology is applied to the same latitude bands in the Southern Hemisphere (80°S in subsection 4.3; 40°S in Appendix A).

##### 4.1 Northern Hemisphere Mid-latitudes

Figure 4 shows the seasonally averaged signature of the different extratropical wave spectrum regions (defined in subsection 2.3, figure 1) at 40°N, as their mean anomaly in the tropopause-based zonal-mean vertical profiles of temperature (left column) and  $N^2$  (right column). All the defined extratropical wave spectrum regions show a mean cold anomaly maximizing at the tropopause (Fig. 4 a and c), and a  $N^2$  increase directly above the tropopause (Fig. 4 b and d), thereby producing a net TIL enhancement. This is also in line with the findings by Pilch Kedzierski et al. (2016), who found the same effect of all equatorial wave types on the tropical TIL, only varying in the amplitude of the mean wave signature. The mean wave signatures in Figure 4 show that extratropical waves enhance the TIL in a very similar manner by tropopause adjustment to the wave signal and the resulting cold anomaly at the tropopause (and a warm anomaly above to a lesser degree).

In Fig. 4 (a-d), the strongest signal belongs to eastward-propagating waves with periods of 4 to 25 days (red lines), in both winter (top row) and summer (bottom row). Baroclinic Rossby waves, the most common wave type occurring at mid-latitudes (with prevailing westerlies during all year at near-tropopause level, therefore their eastward propagation respect to the ground), fit within this  
 415 broadly defined wavenumber-frequency domain. This also explains why the extratropical wave signal is stronger in winter at mid-latitudes, since the mid-latitude jet strength and the baroclinic wave activity both peak there during winter. We also note that quasi-stationary waves (periods of 30-96 days, black and dashed magenta lines) and the  $s=0$  wave (grey line) play a minor role in enhancing the TIL.

420 The total extratropical wave signal (Fig. 4 e and f) at  $40^\circ\text{N}$  is a mean cold anomaly at the tropopause of  $\sim 3.5\text{K}$  and a TIL enhancement of  $\sim 1.6 \times 10^{-4} \text{s}^{-2}$  in winter (red line). In summer (black line) the modulation is weaker: tropopause-centered mean cold anomaly of  $\sim 2.3\text{K}$  and  $\sim 1.1 \times 10^{-4} \text{s}^{-2}$  of TIL enhancement. The spring and autumn wave signatures are similar to the results shown here for winter and summer, respectively. The total extratropical wave signature in NH  
 425 mid-latitude summer has a very similar magnitude compared to the equatorial wave signal obtained by Pilch Kedzierski et al. (2016).

Figure 5a shows the daily evolution of the tropopause-based  $N^2$  profile (2007-2013) at  $40^\circ\text{N}$ . In Fig. 5a the TIL is clearly discernible in winter and into spring with higher  $N^2$  values right above the tropopause, ranging between  $5.5 \times 10^{-4} \text{s}^{-2}$  (orange) and  $6.5 \times 10^{-4} \text{s}^{-2}$  (red). Above the TIL  
 430 in winter, the lowermost stratosphere has a relative minimum in  $N^2$  of  $\sim 3.5 \times 10^{-4} \text{s}^{-2}$  centered at 15km height, and levels higher than 18km have  $N^2$  values of  $\sim 5 \times 10^{-4} \text{s}^{-2}$ . In summer months the tropopause is higher, and although the TIL and the stratospheric  $N^2$  values are separated by a weak relative  $N^2$  minimum (white, blueish sometimes), both layers have  $N^2$  values of  $5-5.5 \times 10^{-4} \text{s}^{-2}$  (yellow, orange sometimes). Fig. 5a agrees with previous climatologies of the mid-latitude  $N^2$  vertical structure (e.g. Birner (2006); Grise et al. (2010)), while also showing its short-term variability  
 435 without time-averages.

Fig. 5b shows the same  $N^2$  profile evolution, but with the daily extratropical wave signal subtracted, therefore displaying the tropopause-based  $N^2$  structures without the instantaneous modulation by planetary to synoptic-scale extratropical waves. Therefore, any TIL observed in Fig. 5b  
 440 should be caused by other processes. It can be observed that the TIL in Fig. 5b is almost completely gone:  $N^2$  right above the tropopause is always lower than the stratospheric values above 18km. However, in winter and spring a very weak relative maximum of  $N^2$  can be observed above the tropopause ( $4-4.5 \times 10^{-4} \text{s}^{-2}$ , white and light-blue colors compared to the  $N^2$  minimum of  $3.5 \times 10^{-4} \text{s}^{-2}$  at 15km height), occasionally reaching  $N^2$  values close to  $5 \times 10^{-4} \text{s}^{-2}$  (sparse light-  
 445 yellow spots) in late winter and spring. In summer, there is no relative  $N^2$  maximum above the tropopause at all in Fig. 5b.

The conclusion that Fig. 5b gives is that most of the mid-latitude TIL is explained by the instantaneous modulation by planetary to synoptic-scale extratropical waves. Other possible sources of TIL enhancement in the extratropics like IGW modulation, wave-mean flow interactions of any  
450 wave type, residual circulation or radiative effects; all together they play a minor role in forming the zonal-mean TIL structure. The TIL enhancement by IGWs (Zhang et al., 2015) can be of importance locally in space and time, but its contribution to the zonal-mean TIL (even if it explained all the structures in Fig. 5b) would be less than the effect of the filtered planetary and synoptic-scale extratropical waves.

455 Separating the different extratropical wave types and their contribution to TIL enhancement is beyond the scope of this study, but of interest for future research. Two questions arise from our results:

1) Which wave type is dominant? Figs. 3 and 4 point towards the baroclinic Rossby wave, the most common and strongest wave type occurring in the extratropics, and we find the biggest signals  
460 in the broad wavenumber-frequency domain that would include this wave type, but this still needs robust confirmation. Our current method would need significant refinement to separate the baroclinic Rossby wave from other wave modes present in the extratropics.

2) Which is the process that leads to the amplification of extratropical waves next to the tropopause level? This is visible in Fig. 3 for all **the wave spectrum regions** defined in subsection 2.3, and  
465 analogous to the near-tropopause amplification of all equatorial wave types in the tropics observed by Pilch Kedzierski et al. (2016). It would be of high interest to know whether this amplification follows Linear Wave Theory (Andrews et al., 1987) or not.

The conclusions from this subsection for 40°N also apply to the Southern Hemisphere. The equivalent analyses for 40°S can be found in Appendix A.

## 470 **4.2 Northern Hemisphere Polar latitudes**

We proceed to apply the same analysis from the previous subsection 4.1 to polar latitudes. Figure 6 shows the seasonal average signature of the different extratropical wave **spectrum regions** (defined in subsection 2.3, Fig. 1) at 80°N, as their mean anomaly in the tropopause-based zonal-mean vertical profiles of temperature (left column) and  $N^2$  (right column). As in mid-latitudes (subsection 4.1),  
475 all the defined extratropical wave **spectrum regions** show a **mean cold anomaly** maximized at the tropopause (Fig. 6 a and c), and a  $N^2$  increase right above the tropopause (Fig. 6 b and d). However, at polar latitudes the seasonality of the extratropical wave forcing is inverted compared to mid-latitudes. The total wave signatures in Fig. 6 e and f are weaker in winter (red line), with a tropopause **mean cold anomaly** of  $\sim 2.6\text{K}$  and a TIL enhancement of  $\sim 1.1 \times 10^{-4} \text{s}^{-2}$ , similar to that found in  
480 mid-latitude summer. In summer (black line), there is a total tropopause **mean cold anomaly** of  $\sim 3.9\text{K}$  and a TIL enhancement of  $\sim 1.9 \times 10^{-4} \text{s}^{-2}$ , similar to that found in mid-latitude winter. **The**

spring and autumn wave signatures at NH polar latitudes are both in between the values for winter and summer shown here.

Note that in Fig. 6 (a-d) the eastward-propagating 4-25 day band (red line) is no longer as dominant as in Fig. 4. This can be explained by the fact that zonal mean westerly winds are weaker at polar latitudes, therefore the wave spectrum does not get Doppler-shifted as much as at mid-latitudes, and more waves are observed to be westward-propagating with respect to the ground. As to why the extratropical wave signature is stronger in polar summer, as opposed to mid-latitudes (stronger in winter), we explain the inverted seasonalities by the position of the jet stream and the baroclinic wave activity, which migrate polewards in summer while being at the mid-latitudes in winter. However, it is still surprising that the total extratropical wave signature on the TIL region is of the same magnitude at mid-latitudes and polar latitudes, despite the opposed seasonal cycles as explained above. Since the meridional temperature gradients and the jet stream are weaker in summer, one would expect the extratropical wave signature on the TIL to follow this tendency. It is possible that extratropical waves at polar regions get amplified near the tropopause and reach the same amplitude as at mid-latitudes (at opposing seasons), but as noted in subsection 4.1 this amplifying mechanism near the tropopause needs further research.

Figure 7a shows the daily evolution of the tropopause-based  $N^2$  profile (2007-2013) at  $80^\circ\text{N}$ . There is a distinct TIL throughout the year, with  $N^2$  values right above the tropopause of  $\sim 5 \times 10^{-4} s^{-2}$  in winter (white to yellow colors) and between  $7-8 \times 10^{-4} s^{-2}$  in summer (brown and black sometimes). Stratospheric  $N^2$  values are around  $4 \times 10^{-4} s^{-2}$  (dark and light blue) at levels within 14-26km height, with increasing  $N^2$  at higher levels. The  $N^2$  structures showed in Fig. 7a (as in Fig. 5a) agree with previous climatologies of the high-latitudes  $N^2$  vertical structure (Birner, 2006; Grise et al., 2010), and the daily temporal resolution shows the high variability associated with sudden stratospheric warmings (SSWs) in the stratosphere. Higher  $N^2$  values in the stratosphere are observed during SSWs, with positive  $N^2$  anomalies propagating downward and reaching the TIL region. The SSWs signals at particular events will be discussed next, since they will be easier to differentiate once the extratropical wave signal is removed in Fig. 7b.

Fig. 7b shows the  $N^2$  profile evolution without the daily extratropical wave signal, displaying the tropopause-based  $N^2$  structures caused by other processes. The TIL in Fig. 7b is significantly weakened without the extratropical wave modulation: in winter it almost disappears, but in summer the TIL is still distinct ( $5-6 \times 10^{-4} s^{-2}$ , yellow and orange) from the background stratospheric  $N^2$  structure (blue). The extratropical wave modulation explains an important part of the TIL's  $N^2$  structure in polar latitudes (a similar amount of  $N^2$  enhancement as in mid-latitudes, with inverted seasonality, Fig. 6), but other sources of TIL enhancement are also present as it can be observed in Fig. 7b (unlike in Fig. 5b for mid-latitudes, where almost no TIL is visible without the extratropical wave signal). Most notably, the removal of the extratropical wave signal makes the time evolution of the vertical  $N^2$  structures in Fig. 7b much smoother compared to Fig. 7a, and allows a clearer

appearance of the downward-propagating signal from SSWs and how it affects the tropopause re-  
520 gion. In Fig. 7b, major SSW events are marked with black arrows (2008, 2009, 2010, 2013), and one  
minor event is marked with a grey arrow in 2012. The major SSW event from February 2007 is not  
marked, since the first 100 days of 2007 are cut off for the analyses in this section.

During major SSWs, the residual circulation is accelerated, and the convergence of its vertical  
component ( $\overline{w^*}$ ) forces a positive temperature anomaly that propagates downward into the lower-  
525 most stratosphere (Andrews et al., 1987). In the study by Wargan and Coy (2016) it was shown  
that  $\overline{w^*}$  convergence is associated with a downward-propagating positive  $N^2$  anomaly as well, that  
enhances the TIL once the SSW signal reaches the tropopause region. Wargan and Coy (2016) cal-  
culated a  $\sim 1.5 \times 10^{-4} s^{-2}$  increase of the zonal-mean  $N^2$  maximum above the tropopause due to the  
2009 major SSW, and slightly lower  $N^2$  increases in other SSW cases. In Fig. 7b, it can be observed  
530 that  $N^2$  right above the tropopause in early 2009 increases from  $\sim 4 \times 10^{-4} s^{-2}$  (blue) before the  
SSW, up to  $\sim 5.5 \times 10^{-4} s^{-2}$  (orange) after the SSW. Also, a positive  $N^2$  anomaly from the 2009  
major SSW can be seen in Fig. 7b propagating downwards throughout the stratosphere (white and  
yellow instead of blue), and the TIL enhancement coincides with the time when this downward-  
propagating anomaly reaches the tropopause region, as well as a marked decrease in the zonal-mean  
535 tropopause height. This perfectly fits the findings of Wargan and Coy (2016). In Fig. 7b the same  
can be observed in the major SSW cases of 2008, 2010 and 2013, although the  $N^2$  anomalies are  
slightly lower than in 2009 which was an exceptionally strong event.

Interestingly, in Fig. 7b we observe the downward-propagating positive  $N^2$  anomaly, TIL en-  
hancement and tropopause lowering in a minor SSW in early 2012, and also during the final warm-  
540 ings of 2011 and 2013. The coherency in time of these signals, and their similarity to the cases  
described by Wargan and Coy (2016) suggests that they are also driven by an acceleration of the  
residual circulation (increased  $\overline{w^*}$  convergence) from the disturbed polar vortex. The 2013 case is  
quite particular: once the major SSW is finished, the polar vortex recovers, the TIL is no longer  
enhanced and the tropopause slowly increases its height; but then there is a strong final warming  
545 event, another downward-propagating  $N^2$  signal, immediate TIL enhancement and a slight lower-  
ing of the zonal-mean tropopause. After this, the zonal-mean tropopause gets steadily higher into  
the summer. In the final warming of 2011 there is an abrupt transition from a strong polar vortex  
to anticyclonic circulation, and the downward-propagating  $N^2$  signal, TIL enhancement and abrupt  
zonal-mean tropopause lowering is also visible in Fig. 7b. In the case of the minor SSW of 2012,  
550 the TIL enhancement and zonal-mean tropopause lowering are also in clear coincidence with the  
disrupted westerlies.

Figure 7b shows evidence, directly from observations, that the TIL is enhanced due to major  
SSWs, and also from other polar vortex disturbances: minor SSWs and abrupt final stratospheric  
warmings. The similarity of our results with Wargan and Coy (2016), who studied major SSWs,  
555 in terms of the time evolution of the  $N^2$  signal, TIL enhancement and tropopause height; suggests

that accelerated residual circulation (increased  $\overline{w^*}$  convergence) is the main contributor to TIL enhancement during all kinds of polar vortex disturbances, not only major SSWs. This would need confirmation with a more detailed study of (non-major) polar vortex disturbances and the associated residual circulation variability.

560 Fig. 6f showed TIL enhancement of  $\sim 1.1 \times 10^{-4} s^{-2}$  by extratropical wave modulation in polar winter. In Fig. 7b, we show that polar vortex disturbances in general can enhance the TIL in winter (major and minor SSWs) and spring (final warmings) with a similar magnitude. The remaining TIL in polar summer in Fig. 7b ( $\sim 5.5 \times 10^{-4} s^{-2}$ , orange) is not explained by extratropical wave modulation, nor by residual circulation. The only other **known mechanism that could enhance the**  
565 **TIL in polar summer** is water vapor radiative cooling of the tropopause (Randel and Wu, 2010; Miyazaki et al., 2010b), but this would also require an additional study to be confirmed.

We also note that the meridional advection of the SSW signals in the lowermost stratosphere could be the cause of the very weak hints of the mid-latitude TIL without the extratropical wave signal found in Fig. 4b, that mainly appears in late winter and spring and was strongest in 2009,  
570 2010 and 2013, coinciding with major SSW events.

Given that the polar vortex behavior affects the TIL more clearly at polar latitudes, we expect more differences between the NH and the SH, since the polar vortex in the SH is much less disturbed than in the NH, and the only **major SSW** observed in the SH happened in 2002.

### 4.3 Southern Hemisphere Polar latitudes

575 Figure 8 is the Southern Hemisphere (SH) equivalent of Fig. 6. The total extratropical wave signal at 80°S (Fig. 8 e and f) is a tropopause **mean cold anomaly** of  $\sim 1.4K$  and a TIL enhancement of  $\sim 0.9 \times 10^{-4} s^{-2}$  in winter (compared to  $\sim 1.4 \times 10^{-4} s^{-2}$  TIL enhancement in the NH in Fig. 6). In summer there is a tropopause **mean cold anomaly** of  $\sim 2.5K$  and  $\sim 1.3 \times 10^{-4} s^{-2}$  of TIL enhancement ( $\sim 1.9 \times 10^{-4} s^{-2}$  in the NH, Fig. 6). The extratropical wave signatures in Fig. 8 show the same  
580 seasonality as in Fig. 6, with stronger (weaker) signals in summer (winter) months, but the overall magnitude of the extratropical wave forcing at polar latitudes is lower in the SH than in the NH. **The spring and autumn wave signatures at SH polar latitudes are similar to the results shown here for winter and summer, respectively.**

The lower extratropical wave activity and the smaller mean signal at the tropopause near the  
585 South pole is explained by the isolation of the SH polar latitudes: no land-sea contrast or high mountain ranges in the meridional direction (less wave sources), and a stronger and more stable polar vortex that does not allow waves to propagate so deep into high latitudes, as opposed to the NH. The behavior of the extratropical wave forcing in SH polar latitudes (Fig. 8) is similar to the NH (Fig. 6) but weaker. In subsection 4.2 (NH polar latitudes) it was shown that, after subtracting  
590 the extratropical wave signal, the TIL enhancement from SSWs (major or minor) and final warmings

could be seen clearly. In the 2007-2013 period, no SSW occurred in the SH, so we only aim to see what is the effect of final warmings.

Figure 9a shows the daily evolution of the tropopause-based  $N^2$  profile at 80°S. There is a clear TIL during summer and into autumn, with  $N^2$  values of  $\sim 7 \times 10^{-4} s^{-2}$  (brown) right above the tropopause. In winter, the TIL is harder to discern, but a weak maximum of  $\sim 4.5 \times 10^{-4} s^{-2}$  (white, light yellow) is present above the winter tropopause. The TIL near the South Pole in winter is known to be very weak or absent (Tomikawa et al., 2009; Pilch Kedzierski et al., 2015). Compared to the NH, the SH polar vortex is stronger, less disturbed during winter, and has a longer lifetime: it breaks later in spring, almost into the summer.

Note that in Fig. 9 the tropopause is higher during winter (unlike in Figs. 5 and 7). This seasonal cycle in the high-latitude SH tropopause agrees with previous climatologies from GPS-RO (Son et al., 2011), and is attributed to the very cold and stable polar vortex (Zängl and Hoinka, 2001) and the seasonal cycle in the strength of the Brewer-Dobson circulation (Yulaeva et al., 1994). Also, there is some indeterminacy in the exact height of the thermal tropopause, since the background temperature lapse-rate in SH high-latitudes is close to the WMO lapse-rate tropopause criterion (WMO, 1957) of 2K/km for several kilometers in the upper troposphere during winter. We discuss the downward-propagating signal of the SH polar vortex breakup next.

Fig. 9b shows the  $N^2$  profile evolution without the daily extratropical wave signal, displaying the tropopause-based  $N^2$  structures caused by other processes. In summer, the TIL is significantly weaker but clearly present in Fig. 9b. In winter, the TIL cannot be detected without the extratropical wave signal, and the vertical  $N^2$  structures are smoother and enable a clearer view of the downward-propagating  $N^2$  signal from the SH vortex breakup in late spring. Once the signal reaches the tropopause region, there is an abrupt increase in  $N^2$  right above the tropopause, from values of  $\sim 4 \times 10^{-4} s^{-2}$  (blue) to  $\sim 5.5 \times 10^{-4} s^{-2}$  (yellow-orange), in line with the findings of Wargan and Coy (2016) and our previous subsection 4.2 and Fig. 7b. Even a slight and short-lived relative minimum in tropopause height can be observed with the arrival of the vortex breakup signal. Note that in Fig. 9b, no TIL is discernible until the downward-propagating  $N^2$  signal from the SH polar vortex breakup arrives. For example, the contrast between the summers of 2011/12 and 2012/13: in the first summer, the signal reaches the tropopause region right at the beginning of 2012, and the TIL is observed since; whereas in the next summer the polar vortex breaks up early, and the strong TIL is observed more than a month before the beginning of 2013.

Later in the summer, the TIL generally reaches  $N^2$  values of  $\sim 6 \times 10^{-4} s^{-2}$  every year in Fig. 9b. As in the previous subsection 4.2, we also suggest that the remaining TIL in Fig. 9b in summer is due to water vapor radiative effects which would need further study.

625 **5 Discussion**

In subsection 2.4 we introduced a new TIL enhancing mechanism, section 3 showed that gridded COSMIC GPS-RO observations are able to capture it, and throughout section 4 we quantified the importance of extratropical wave modulation in explaining the observed mid- and polar latitude TIL strength and variability. Within this section we will discuss how the wave modulation mechanism  
630 relates to previously proposed TIL enhancing mechanisms, since it can integrate several of them rather than being a completely separate dynamical feature of the tropopause region.

First of all, it is important to clarify what our wave modulation mechanism and the filtered wave anomalies represent exactly. The waves are defined as space-time harmonics of positive-negative (T or  $N^2$ ) anomalies whose sum in the ground-based mean profile is zero, thereby not affecting the  
635 background T and  $N^2$  profile at all. They represent the adiabatic and transient dynamical effect of the wave: once the wave (as the space-time harmonic) leaves the tropopause region or dissipates, it is not filtered out and therefore would no longer influence the tropopause region, which would then be back to its background state. The key detail about this mechanism lies in that, in order to have a significant role in enhancing the TIL, it needs of a constant presence of high-amplitude waves in the  
640 extratropical tropopause region. Indeed, GPS-RO observations show this to be the case (see sections 3 and 4).

Another important point to take into account is: what is included within the concept of 'Atmospheric Wave'? Traveling and transient T and  $N^2$  anomalies are just a part of the wave that our method is able to quantify, but there are horizontal and vertical motions associated with the wave as  
645 well, which can influence water vapor transport and induce the formation of clouds, in turn influencing the local radiative budget and heat fluxes. Also, the waves can interact with the mean flow while breaking and/or dissipating. All of this cannot be observed with GPS-RO measurements, nor quantified with our filtering method.

The benefit of our method is that it separates the transient and adiabatic effect of the extratropical  
650 waves (that drive variability around the background T and  $N^2$  profiles) from the rest of diabatic processes, associated with the wave or not, whose imprint is present at longer space and time-scales (and can shape the background T and  $N^2$  profiles). The latter are still present in Figs. 7b and 9b once the wave signals are subtracted, and agree well with previous literature about the role of the accelerated Brewer-Dobson circulation in enhancing the polar TIL during SSWs (Wargan and Coy,  
655 2016) and water vapor radiative effects in enhancing the polar summer TIL (Randel and Wu, 2010; Miyazaki et al., 2010b).

The wave signature on the tropopause-based, zonal mean T and  $N^2$  profiles has a similar magnitude in polar summer and mid-latitude winter (Figs. 4 and 6). At mid-latitudes (Figs. 5b and A2b), the filtered wave signals seem to be responsible for most of the observed TIL. How does this fit to  
660 previously proposed TIL enhancing mechanisms? We suggest that, rather than being a completely separate dynamical feature, several mechanisms proposed in earlier literature are integrated within

our wave modulation mechanism and the filtered wave signals. We will start discussing the dynamical ones and finish with processes related to radiation.

665 The cyclones and anticyclones embedded within the Rossby wave travel in the same wavenumber-frequency domain. The vertical convergence and isentrope packing happening above the anticyclone and enhancing the TIL (Wirth, 2003, 2004) would therefore be captured by our filters as a positive  $N^2$  anomaly (the closer isentropes imply an increased potential temperature gradient). The experiments by Wirth (2003, 2004) involved very idealized axisymmetric vortices, which do not form often in the real atmosphere, but our filtering method is very flexible in capturing the vertical  
670 structure of the waves (see subsections 2.3 and 2.4) and the gridded GPS-RO observations capture the lower-higher tropopauses associated with the traveling cyclones-anticyclones, regardless of their symmetry or complexity.

Erler and Wirth (2011) pointed out the role of wave breaking in forming a stronger TIL in their baroclinic life cycle experiments. During the onset of a wave breaking event, the amplitude of the  
675 baroclinic wave is at its highest, and its modulation of the tropopause region and the TIL is captured with our method. Our results suggest that this effect is more important than the wave-mean flow interactions associated with the wave breaking, whose more permanent effect should be visible in Figs. 4b and A2b after subtracting the wave signals.

IGWs and GWs can locally modulate  $N^2$  near the tropopause and be important for TIL enhancement (Kunkel et al., 2014; Zhang et al., 2015), but our results show that the zonal-mean seasonal  
680 TIL is dominated by waves of synoptic and planetary scales.

Regarding radiation, recent modeling studies highlighted the importance of including diabatic processes related to water vapor and clouds, apart from dynamics, in order to explain the mid-latitude  
685 TIL (Ferreira et al., 2016; Kunkel et al., 2016). Particularly, the baroclinic life cycle experiments by Kunkel et al. (2016) that included diabatic effects from water vapor and clouds showed a faster deepening of the wave and strengthening of the TIL, along with an increase in the cross-tropopause gradient of water vapor which would in turn increase radiative cooling of the tropopause.

We propose that radiation from water vapor and clouds could enhance the TIL in two different ways: **1)** directly influencing the UTLS background T and  $N^2$  profiles, as probably is the case for  
690 the polar summer TIL which is supported by previous literature (Randel and Wu, 2010; Miyazaki et al., 2010b), and Figs. 7b and 9b; and **2)** by also setting up a radiative-dynamical feedback that amplifies atmospheric waves near the tropopause which would explain why our filtered wave anomalies are maximized near the tropopause (Fig. 3) and the absence of a TIL in Figs. 5b and A2b after removing the wave signals, while also fitting with the results by Ferreira et al. (2016) and Kunkel et al.  
695 (2016). Radiation would then be of importance for enhancing baroclinic wave growth, among other factors that trigger the wave and its growth near the tropopause. Further research needs to be done in order to verify and disclose the importance of such radiative-dynamical feedback.

In any case, we stress that the TIL enhancement by the wave modulation mechanism (described in subsection 2.4) is ultimately done by the atmospheric wave in a transient and adiabatic way as shown throughout section 4. We suggest that the wave modulation mechanism integrates the effects of different processes postulated in earlier TIL literature, whose exact roles need further assessment. The step forward done by our study is to identify the total influence of planetary and synoptic-scale waves on the observed TIL strength, and its transient and adiabatic nature.

## 6 Concluding Remarks

Our study used a simplified method to extract the total extratropical (planetary to synoptic-scale) wave signal from gridded COSMIC GPS-RO profiles. By tropopause-based zonal averaging of these signals at certain latitude bands, we were able to quantify how much of the extratropical TIL at mid- and polar latitudes is explained by the instantaneous modulation of the tropopause region by the planetary and synoptic-scale waves. By subtracting the extratropical wave signal, we show how much of the TIL is left due to other processes.

We found that extratropical wave modulation explains almost all of the observed TIL strength at mid-latitudes in both hemispheres (Figs. 5 and A2). Therefore we conclude that wave-mean flow interactions, inertia-gravity waves or the residual circulation are of minor importance as TIL enhancing mechanisms there.

At polar regions, extratropical wave modulation is dominant as well in explaining the TIL strength, but there is also a clear signal from SSWs, major and minor, in the Northern Hemisphere, and final warmings in both hemispheres (Figs. 7 and 9). The similarity in the time evolution of all signals from the disturbed polar vortexes in both hemispheres suggests that they are forced by the same mechanism:  $\overline{w^*}$  convergence from accelerated residual circulation as in the major SSW study by Wargan and Coy (2016).

Also, part of the polar summer TIL strength is not explained by extratropical wave modulation nor by residual circulation. We suggest that the only other known mechanism that could enhance the polar summer TIL is water vapor radiative cooling of the tropopause (Randel and Wu, 2010; Miyazaki et al., 2010b), which requires additional study to be confirmed.

Two questions arise from our results: **1)** what are the separate roles of the different planetary and synoptic-scale wave types within the total extratropical wave modulation of the TIL, and **2)** which is the mechanism for wave amplification near the tropopause as seen in Fig. 3 (see section 5).

Our study, working only with COSMIC GPS-RO observations, has identified and quantified an important mechanism for extratropical TIL enhancement: extratropical wave modulation, which is dominant in the extratropics and especially at mid-latitudes. We suggest that the remaining TIL in polar regions can be explained by accelerated residual circulation from polar vortex disturbances

(given the similarities of our results with Wargan and Coy (2016)) and water vapor radiative effects in polar summer, although these would need to be confirmed by additional studies.

### Appendix A: Wave modulation of the TIL in SH Mid-latitudes

735 Figure A1 is the Southern Hemisphere equivalent of Fig. 4 (which was for 40°N). The signatures of the different extratropical waves in Fig. A1 lead to the same conclusions for the SH mid-latitudes: all defined waves show a net **cold anomaly** maximizing at the tropopause, a slight **mean warm anomaly** above it, and a net  $N^2$  increase directly above the tropopause (Fig. A1 a-d). The strongest wave signal belongs to eastward-propagating waves with periods of 4 to 25 days (red lines), which is even  
740 more dominant in Fig. A1 than in Fig. 4 due to the stronger westerlies found in the SH. Quasi-stationary waves (periods of 30-96 days, black and dashed magenta lines) and the s=0 wave (grey line) play a minor role in enhancing the TIL in both hemispheres.

The total extratropical wave signal (Fig. A1 e-f) at 40°S is a  $\sim 3.6\text{K}$  colder tropopause in the seasonal zonal-mean, tropopause-based profile, and a TIL enhancement of  $\sim 1.7 \times 10^{-4} \text{s}^{-2}$  in winter  
745 (red line). In summer (black line) the modulation is weaker: tropopause **mean cold anomaly** of  $\sim 3.0\text{K}$  and  $\sim 1.4 \times 10^{-4} \text{s}^{-2}$  of TIL enhancement. The total extratropical wave signature in SH mid-latitudes has the same winter-summer seasonality as the NH, and a slightly higher magnitude throughout the year. **The spring and autumn wave signatures are similar to the results shown here for winter and summer, respectively.**

750 Figure A2 compares the daily evolution of the zonal-mean, tropopause-based vertical  $N^2$  profile at 40°S, with (Fig. A2a) and without the extratropical wave signal (Fig. A2b). Fig. A2 is the SH equivalent of Fig. 5, and also leads to the same conclusions: there is a distinct TIL in Fig. A2a throughout the year ( $\sim 6 \times 10^{-4} \text{s}^{-2}$ , orange-red in winter;  $\sim 5 \times 10^{-4} \text{s}^{-2}$  yellow in summer), which is almost completely gone once the daily extratropical wave signal is subtracted. The weak hints of  
755 a TIL seen in Fig. 5b are even weaker in Fig. A2b, suggesting that other TIL enhancing processes play an even **smaller** role in the SH. We conclude from Fig. A2 that the TIL modulation by planetary and synoptic-scale waves explains most of the TIL strength in the tropopause-based  $N^2$  structure at mid-latitudes also in the SH.

The findings of subsection 4.1 (NH mid-latitudes, Figs. 4 and 5) also apply to the SH (Figs. A1  
760 and A2) in a nearly-coincident way.

*Acknowledgements.* This study was completed within the Helmholtz-University Young Investigators Group NATHAN project, funded by the Helmholtz Association through the president's Initiative and Networking Fund and the GEOMAR Helmholtz-Centre for Ocean Research in Kiel. We thank the ECMWF data server for the freely available ERA-Interim data; and UCAR for the COSMIC, satellite missions' temperature profiles.

765 The assistance accessing different datasets and discussions with Sandro Lubis, Wuke Wang and Sebastian Wahl are also appreciated.

## References

- Andrews, D. G., Holton, J. R., and Leovy, C. B.: Middle atmosphere dynamics, International Geophysics Series, Vol. 40, Academic Press, 1987.
- 770 Anthes, R. A., Bernhardt, P. A., Chen, Y., Cucurull, L., Dymond, K. F., Ector, D., Healy, S. B., Ho, S.-P., Hunt, D. C., Kuo, Y.-H., Liu, H., Manning, K., McCormick, C., Meehan, T. K., Randel, W. J., Rocken, C., Schreiner, W. S., Sokolovskiy, S. V., Syndergaard, S., Thompson, D. C., Trenberth, K. E., Wee, T.-K., Yen, N. L., and Zeng, Z.: The COSMIC/FORMOSAT-3 Mission: Early Results, *Bulletin of the American Meteorological Society*, 89, 313, doi:10.1175/BAMS-89-3-313, 2008.
- 775 Birner, T.: Fine-scale structure of the extratropical tropopause region, *Journal of Geophysical Research (Atmospheres)*, 111, D04104, doi:10.1029/2005JD006301, 2006.
- Birner, T.: Residual Circulation and Tropopause Structure, *Journal of Atmospheric Sciences*, 67, 2582–2600, doi:10.1175/2010JAS3287.1, 2010.
- Birner, T., Dörnbrack, A., and Schumann, U.: How sharp is the tropopause at midlatitudes?, *Geophysical Research Letters*, 29, 1700, doi:10.1029/2002GL015142, 2002.
- 780 Dee, D. P., Uppala, S. M., Simmons, A. J., Berrisford, P., Poli, P., Kobayashi, S., Andrae, U., Balmaseda, M. A., Balsamo, G., Bauer, P., Bechtold, P., Beljaars, A. C. M., van de Berg, L., Bidlot, J., Bormann, N., Delsol, C., Dragani, R., Fuentes, M., Geer, A. J., Haimberger, L., Healy, S. B., Hersbach, H., Hólm, E. V., Isaksen, I., Kållberg, P., Köhler, M., Matricardi, M., McNally, A. P., Monge-Sanz, B. M., Morcrette, J.-J., Park, B.-K., Peubey, C., de Rosnay, P., Tavolato, C., Thépaut, J.-N., and Vitart, F.: The ERA-Interim reanalysis: configuration and performance of the data assimilation system, *Quarterly Journal of the Royal Meteorological Society*, 137, 553–597, doi:10.1002/qj.828, 2011.
- Erlner, A. R. and Wirth, V.: The Static Stability of the Tropopause Region in Adiabatic Baroclinic Life Cycle Experiments, *Journal of Atmospheric Sciences*, 68, 1178–1193, doi:10.1175/2010JAS3694.1, 2011.
- 790 Ferreira, A. P., Castanheira, J. M., and Gimeno, L.: Water vapour stratification and dynamical warming behind the sharpness of the Earth’s midlatitude tropopause, *Quarterly Journal of the Royal Meteorological Society*, 142, 957–970, doi:10.1002/qj.2697, 2016.
- Geggelman, A., Hoor, P., Pan, L. L., Randel, W. J., Hegglin, M. I., and Birner, T.: The Extratropical Upper Troposphere and Lower Stratosphere, *Reviews of Geophysics*, 49, RG3003, doi:10.1029/2011RG000355, 795 2011.
- Grise, K. M., Thompson, D. W. J., and Birner, T.: A Global Survey of Static Stability in the Stratosphere and Upper Troposphere, *Journal of Climate*, 23, 2275–2292, doi:10.1175/2009JCLI3369.1, 2010.
- Hegglin, M. I., Boone, C. D., Manney, G. L., and Walker, K. A.: A global view of the extratropical tropopause transition layer from Atmospheric Chemistry Experiment Fourier Transform Spectrometer O<sub>3</sub>, H<sub>2</sub>O, and 800 CO, *Journal of Geophysical Research (Atmospheres)*, 114, D00B11, doi:10.1029/2008JD009984, 2009.
- Kunkel, D., Hoor, P., and Wirth, V.: Can inertia-gravity waves persistently alter the tropopause inversion layer?, *Geophysical Research Letters*, 41, 7822–7829, doi:10.1002/2014GL061970, 2014.
- Kunkel, D., Hoor, P., and Wirth, V.: The tropopause inversion layer in baroclinic life-cycle experiments: the role of diabatic processes, *Atmospheric Chemistry and Physics*, 16, 541–560, doi:10.5194/acp-16-541-2016, 805 2016.

- Kunz, A., Konopka, P., Müller, R., Pan, L. L., Schiller, C., and Rohrer, F.: High static stability in the mixing layer above the extratropical tropopause, *Journal of Geophysical Research (Atmospheres)*, 114, D16305, doi:10.1029/2009JD011840, 2009.
- 810 Kursinski, E. R., Hajj, G. A., Schofield, J. T., Linfield, R. P., and Hardy, K. R.: Observing Earth's atmosphere with radio occultation measurements using the Global Positioning System, *Journal of Geophysical Research: Atmospheres*, 102, 23 429–23 465, doi:10.1029/97JD01569, 1997.
- Miyazaki, K., Watanabe, S., Kawatani, Y., Sato, K., Tomikawa, Y., and Takahashi, M.: Transport and Mixing in the Extratropical Tropopause Region in a High-Vertical-Resolution GCM. Part II: Relative Importance of Large-Scale and Small-Scale Dynamics, *Journal of Atmospheric Sciences*, 67, 1315–1336, 815 doi:10.1175/2009JAS3334.1, 2010a.
- Miyazaki, K., Watanabe, S., Kawatani, Y., Tomikawa, Y., Takahashi, M., and Sato, K.: Transport and Mixing in the Extratropical Tropopause Region in a High-Vertical-Resolution GCM. Part I: Potential Vorticity and Heat Budget Analysis, *Journal of Atmospheric Sciences*, 67, 1293–1314, doi:10.1175/2009JAS3221.1, 2010b.
- 820 Pilch Kedzierski, R., Matthes, K., and Bumke, K.: Synoptic-scale behavior of the extratropical tropopause inversion layer, *Geophysical Research Letters*, 42, 10,018–10,026, doi:10.1002/2015GL066409, 2015GL066409, 2015.
- Pilch Kedzierski, R., Matthes, K., and Bumke, K.: The tropical tropopause inversion layer: variability and modulation by equatorial waves, *Atmospheric Chemistry and Physics*, 16, 11 617–11 633, doi:10.5194/acp-16-11617-2016, 2016.
- 825 Randel, W. J. and Wu, F.: Kelvin wave variability near the equatorial tropopause observed in GPS radio occultation measurements, *Journal of Geophysical Research (Atmospheres)*, 110, D03102, doi:10.1029/2004JD005006, 2005.
- Randel, W. J. and Wu, F.: The Polar Summer Tropopause Inversion Layer, *Journal of Atmospheric Sciences*, 67, 2572–2581, doi:10.1175/2010JAS3430.1, 2010.
- 830 Randel, W. J., Wu, F., and Forster, P.: The Extratropical Tropopause Inversion Layer: Global Observations with GPS Data, and a Radiative Forcing Mechanism, *Journal of Atmospheric Sciences*, 64, 4489, doi:10.1175/2007JAS2412.1, 2007.
- Schmidt, T., Cammas, J.-P., Smit, H. G. J., Heise, S., Wickert, J., and Haser, A.: Observational characteristics of the tropopause inversion layer derived from CHAMP/GRACE radio occultations and MOZAIC aircraft 835 data, *Journal of Geophysical Research (Atmospheres)*, 115, D24304, doi:10.1029/2010JD014284, 2010.
- Schreck, C.: Extract equatorial waves by filtering in the Wheeler-Kiladis wavenumber-frequency domain., [https://www.ncl.ucar.edu/Document/Functions/User\\_contributed/kf\\_filter.shtml](https://www.ncl.ucar.edu/Document/Functions/User_contributed/kf_filter.shtml), 2009.
- Sjoberg, J. P. and Birner, T.: Stratospheric Wave-Mean Flow Feedbacks and Sudden Stratospheric Warmings in a Simple Model Forced by Upward Wave Activity Flux, *Journal of Atmospheric Sciences*, 71, 4055–4071, 840 doi:10.1175/JAS-D-14-0113.1, 2014.
- Son, S.-W. and Polvani, L. M.: Dynamical formation of an extra-tropical tropopause inversion layer in a relatively simple general circulation model, *Geophysical Research Letters*, 34, L17806, doi:10.1029/2007GL030564, 2007.

- 845 Son, S.-W., Tandon, N. F., and Polvani, L. M.: The fine-scale structure of the global tropopause derived from COSMIC GPS radio occultation measurements, *Journal of Geophysical Research (Atmospheres)*, 116, D20113, doi:10.1029/2011JD016030, 2011.
- Tomikawa, Y., Nishimura, Y., and Yamanouchi, T.: Characteristics of Tropopause and Tropopause Inversion Layer in the Polar Region, *SOLA*, 5, 141–144, doi:10.2151/sola.2009-036, 2009.
- 850 Wargan, K. and Coy, L.: Strengthening of the Tropopause Inversion Layer during the 2009 Sudden Stratospheric Warming: A MERRA-2 Study, *Journal of Atmospheric Sciences*, 73, 1871–1887, doi:10.1175/JAS-D-15-0333.1, 2016.
- Wheeler, M. and Kiladis, G. N.: Convectively Coupled Equatorial Waves: Analysis of Clouds and Temperature in the Wavenumber-Frequency Domain., *Journal of Atmospheric Sciences*, 56, 374–399, doi:10.1175/1520-0469(1999)056<0374:CCEWAO>2.0.CO;2, 1999.
- 855 Wirth, V.: Static Stability in the Extratropical Tropopause Region., *Journal of Atmospheric Sciences*, 60, 1395–1409, doi:10.1175/1520-0469(2003)060<1395:SSITET>2.0.CO;2, 2003.
- Wirth, V.: A dynamical mechanism for tropopause sharpening, *Meteorologische Zeitschrift*, 13, 477–484, doi:10.1127/0941-2948/2004/0013-0477, 2004.
- Wirth, V. and Szabo, T.: Sharpness of the extratropical tropopause in baroclinic life cycle experiments, *Geophysical Research Letters*, 34, 2809, doi:10.1029/2006GL028369, 2007.
- 860 WMO: Meteorology-A three-dimensional science, *WMO Bull.*, 6, 134–138, 1957.
- WMO: Guide to Meteorological Instruments and Methods of Observation, 6th ed. WMO No. 8, 1996.
- Yulaeva, E., Holton, J. R., and Wallace, J. M.: On the Cause of the Annual Cycle in Tropical Lower-Stratospheric Temperatures., *Journal of Atmospheric Sciences*, 51, 169–174, doi:10.1175/1520-0469(1994)051<0169:OTCOTA>2.0.CO;2, 1994.
- 865 Zängl, G. and Hoinka, K. P.: The Tropopause in the Polar Regions., *Journal of Climate*, 14, 3117–3139, doi:10.1175/1520-0442(2001)014<3117:TTITPR>2.0.CO;2, 2001.
- Zhang, Y., Zhang, S., Huang, C., Huang, K., Gong, Y., and Gan, Q.: The interaction between the tropopause inversion layer and the inertial gravity wave activities revealed by radiosonde observations at a midlatitude station, *Journal of Geophysical Research: Atmospheres*, 120, 8099–8111, doi:10.1002/2015JD023115, 2015.
- 870

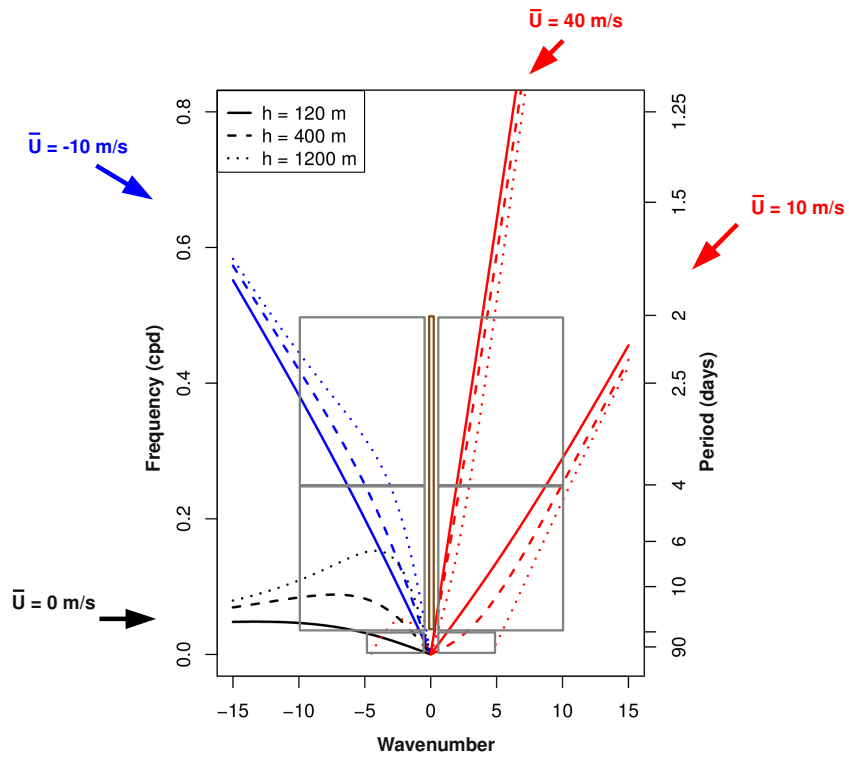


**Figure 1.** Dispersion curves for forced Planetary Waves at 50°N under different mean zonal wind regimes (line colors, winds specified outside the diagram), and differentiating equivalent depths (line type, top-left box). Filter bounds in the wavenumber-frequency domain are shown as grey boxes (brown for wavenumber zero).

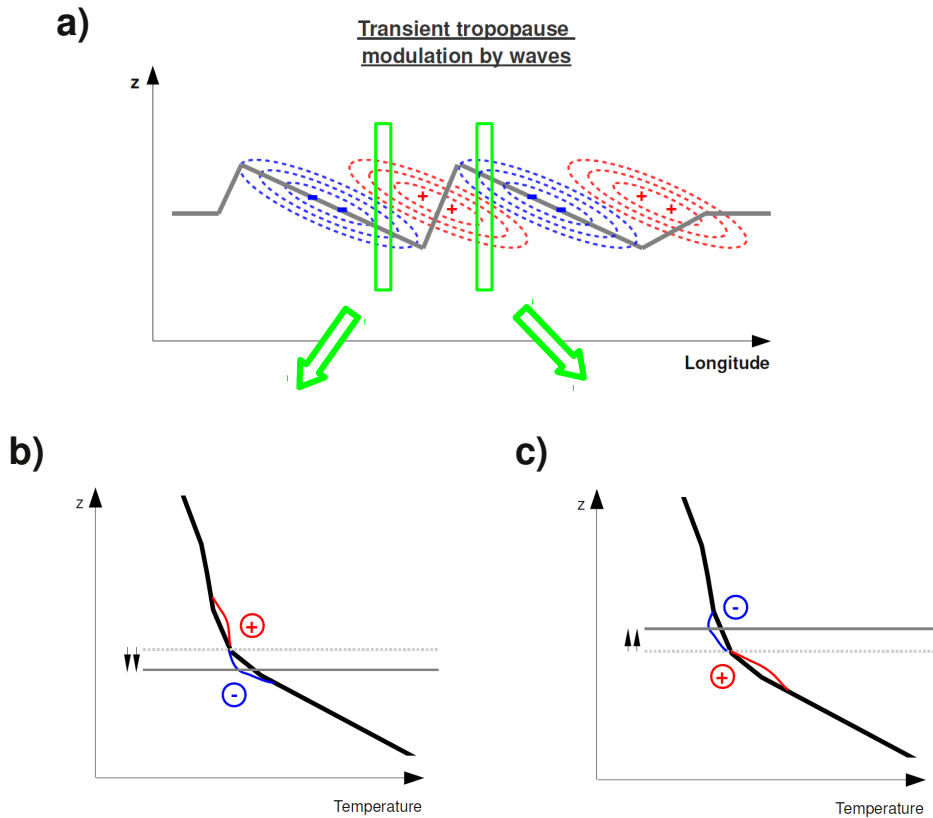


**Figure 2.** **a)** Schematic of transient tropopause modulation by an idealized wave with westward vertical tilt, as a snapshot of the wave's temperature anomalies (dashed contours: positive red, negative blue) and the undulating tropopause (thick and solid grey line). Green boxes represent the local samples for the bottom row. **b)** Ground-based mean temperature profile (thick black line, similar to the mid-latitude profile from Birner (2006), Fig. 8), zonal-mean tropopause height (grey dashed line), the local wave temperature anomalies superimposed on the zonal-mean temperature profile (positive red, negative blue), and the resulting locally lower tropopause (solid grey line, double arrow). **c)** same as (b) but with the opposite sign of the anomalies and a locally higher tropopause.

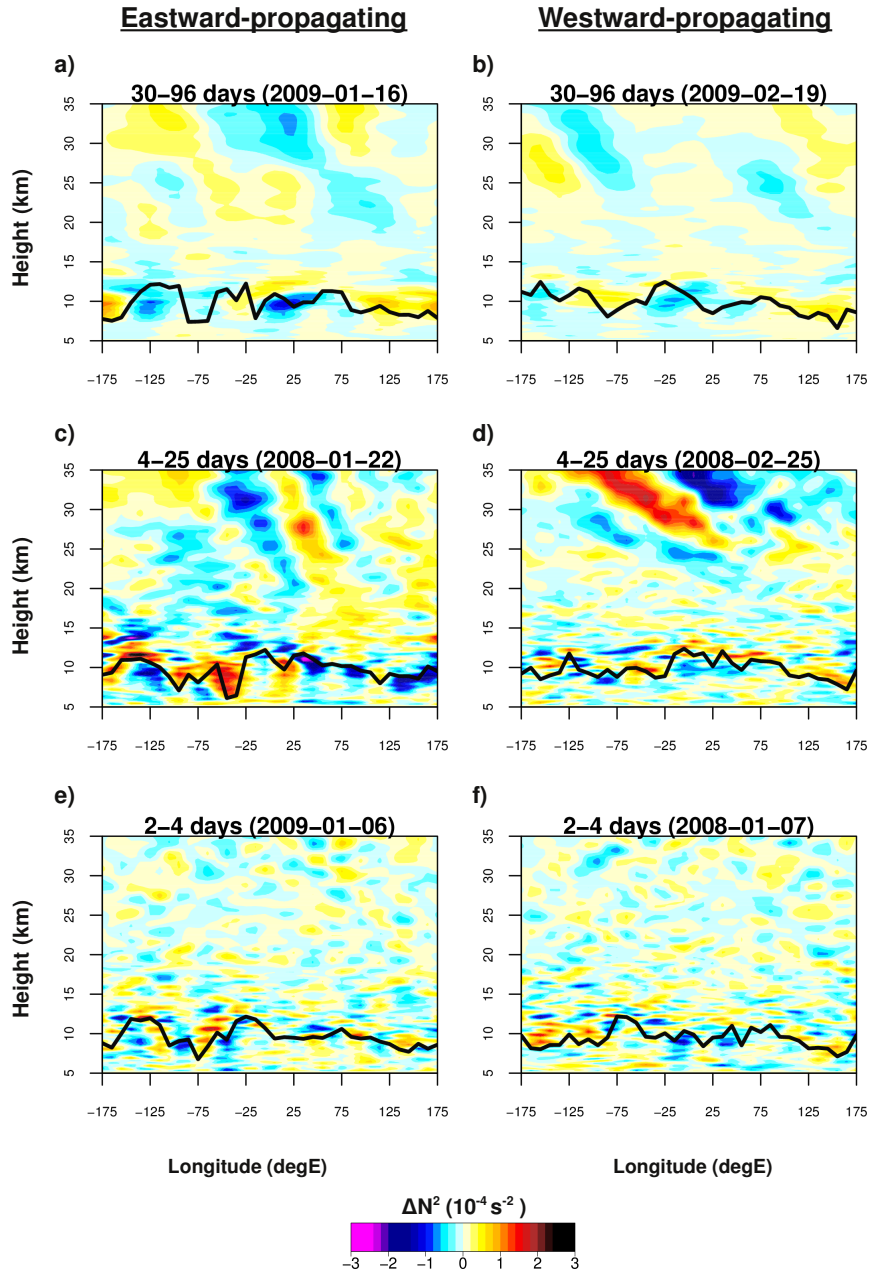


**Figure 3.** Longitude-height snapshots of the  $N^2$  anomalies of the different wave spectrum regions at certain dates, for the 50°N latitude band. The wave spectrum regions correspond to the wavenumber-frequency domains defined in Fig. 1, except for wavenumber zero. Left column are eastward-propagating waves, right column are westward-propagating waves, and their periods are specified along with the date. The black line denotes the thermal tropopause from GPS-RO profiles.

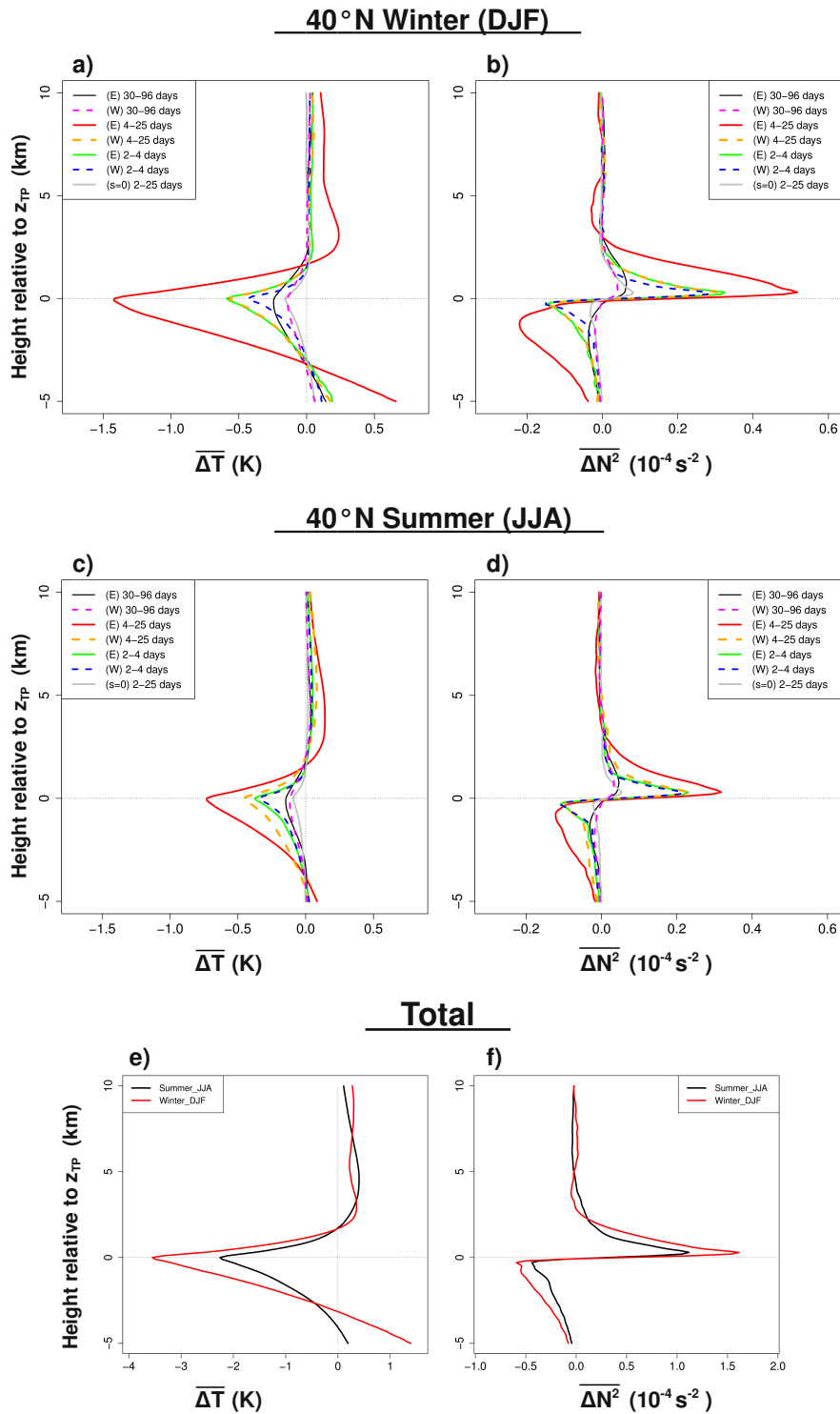


**Figure 4.** Average signature of the different wave spectrum regions at 40°N, as the mean anomaly in the zonal-mean vertical profiles of temperature ( $\overline{\Delta T}$ , left column) and static stability ( $\overline{\Delta N^2}$ , right column). Top row (a and b) for winter (DJF), middle row (c and d) for summer (JJA). Bottom row (e and f) compares the total seasonal wave signatures.

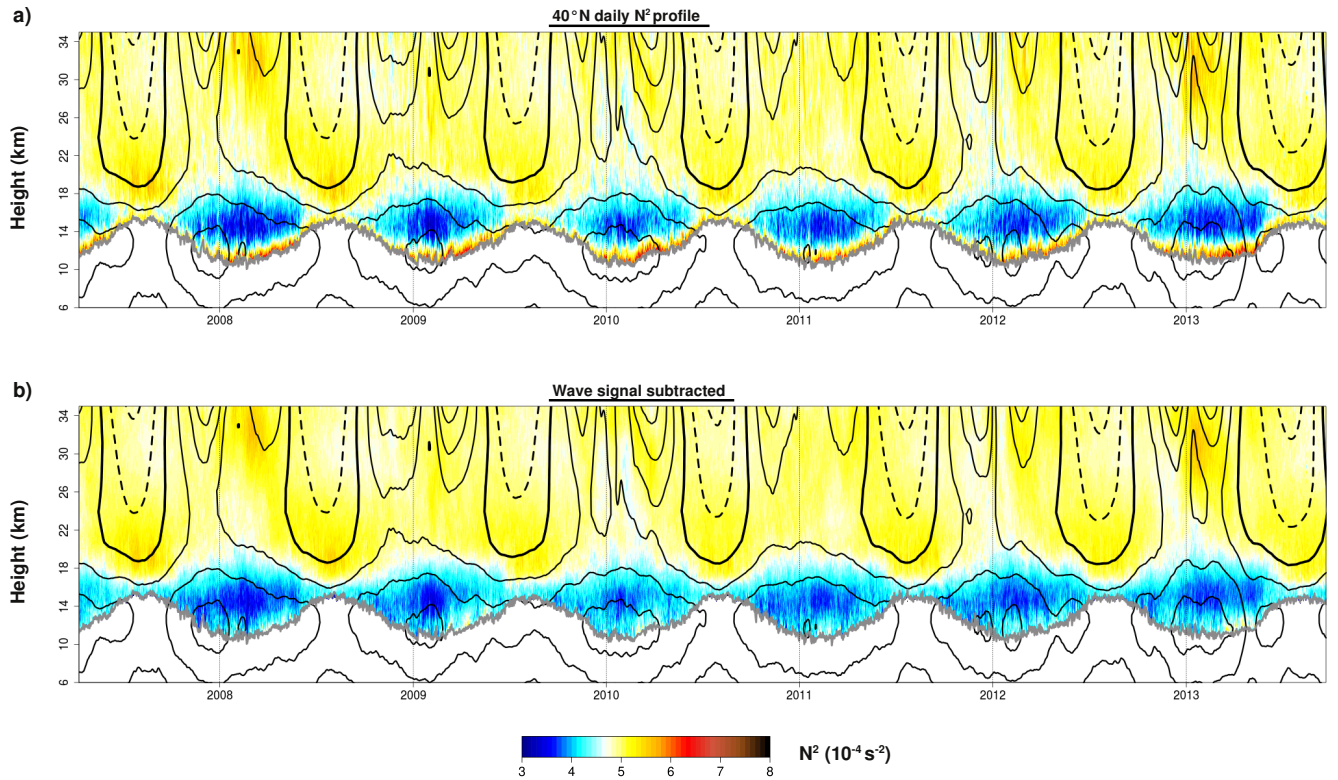
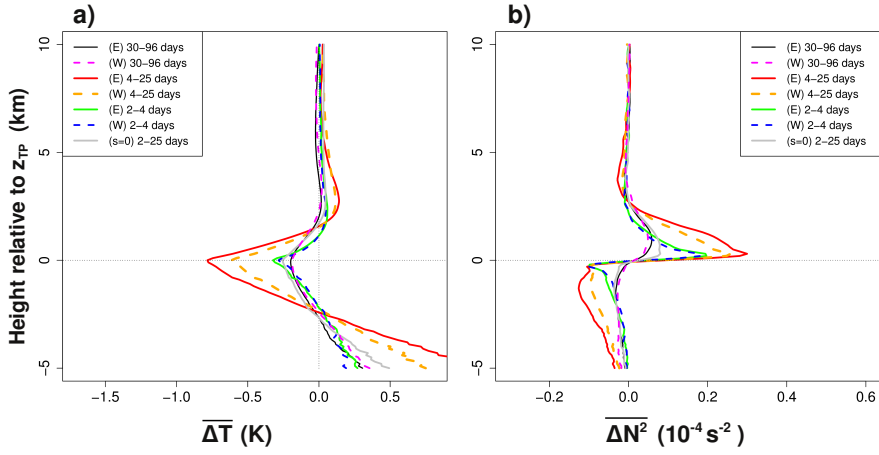
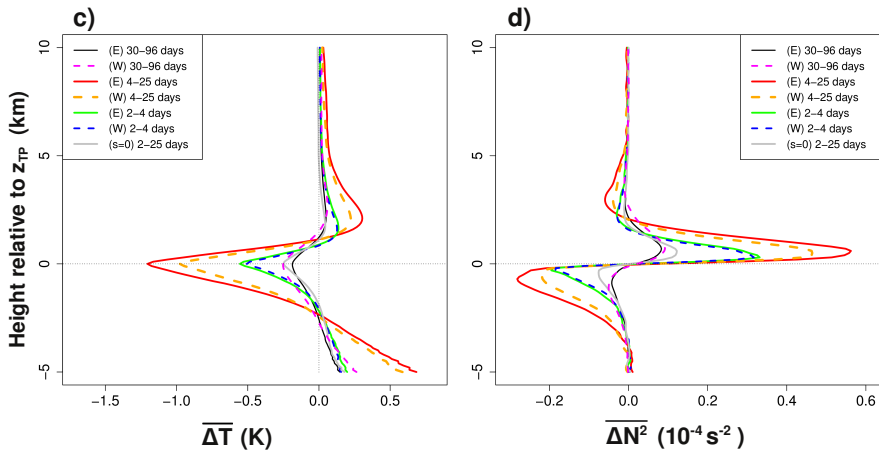


**Figure 5.** a) Daily evolution of the tropopause-based, 40°N zonal mean  $N^2$  vertical profile between 2007-2013 (colors) from COSMIC GPS-RO profiles. The grey line denotes the tropopause height ( $TP_z$ ). Thin black contours denote positive (westerly) mean zonal wind, with a thicker contour for the zero line, dashed contours for negative (easterly) winds, and a 10m/s separation. Winds were obtained from the ERA-Interim reanalysis. To improve visibility, the winds are displayed with a running mean of  $\pm 15$  days. No running mean is applied to the  $N^2$  vertical profile or  $TP_z$  in order to allow the subtraction of the extratropical wave signal. Note that tropospheric  $N^2$  values are not included in the color scale and therefore left blank. b) Same as in Fig. 5a, but the daily wave signal has been subtracted from the  $N^2$  vertical profile.

### 80°N Winter (DJF)



### 80°N Summer (JJA)



### Total

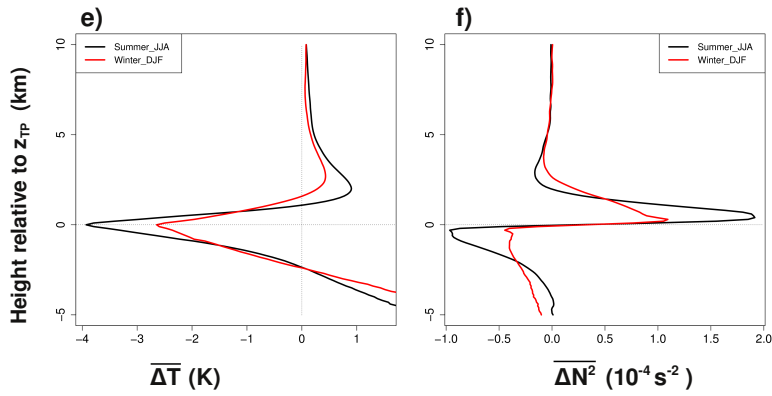
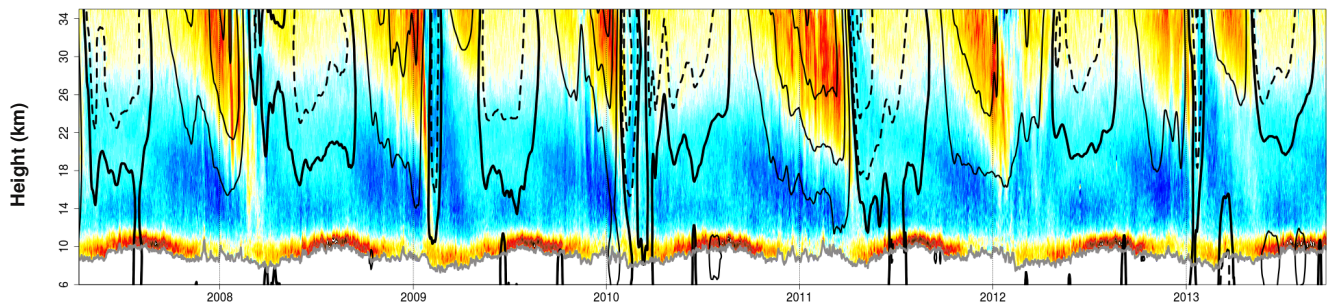
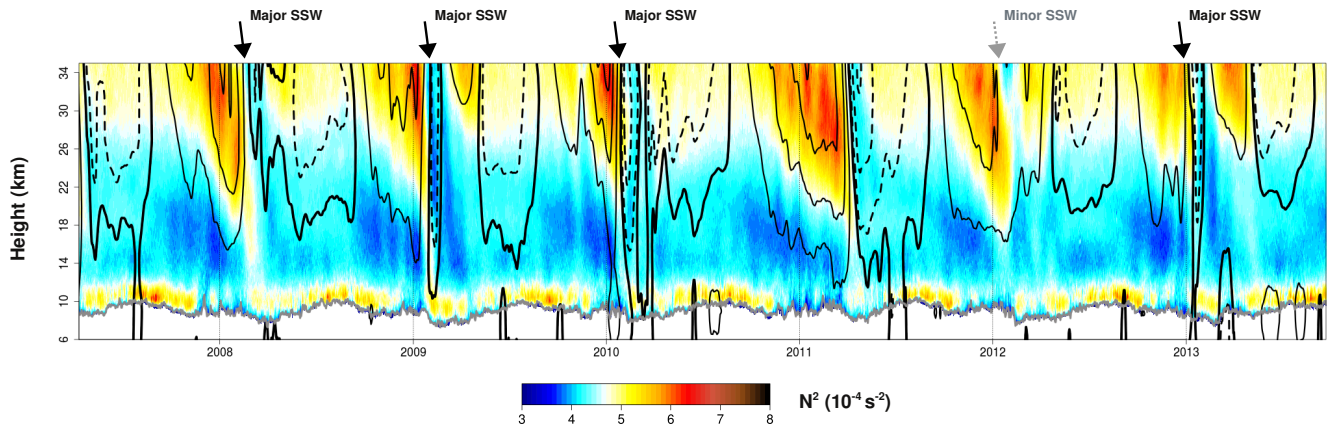


Figure 6. As in Fig. 4, but for 80°N.

a) 80°N daily  $N^2$  profile



b) Wave signal subtracted



**Figure 7.** As in Fig. 5, but for 80°N. Major and minor SSWs are marked above Fig. 7b. First easterly wind contour (dashed line) at -3m/s for better visibility. The rest of wind contours are 10m/s intervals as in Fig. 5.

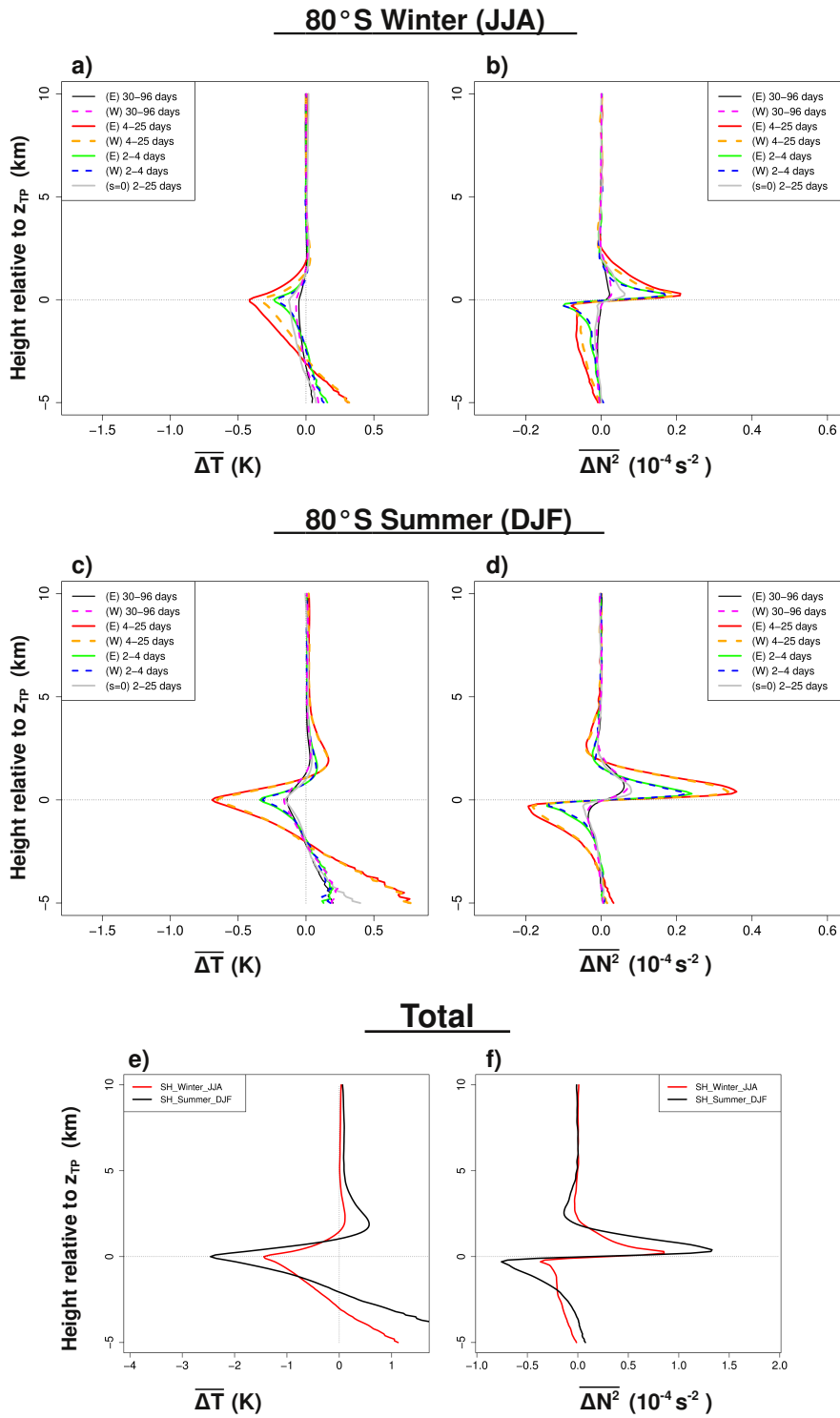


**Figure 8.** As in Figs. 4 and 6, but for 80°S.

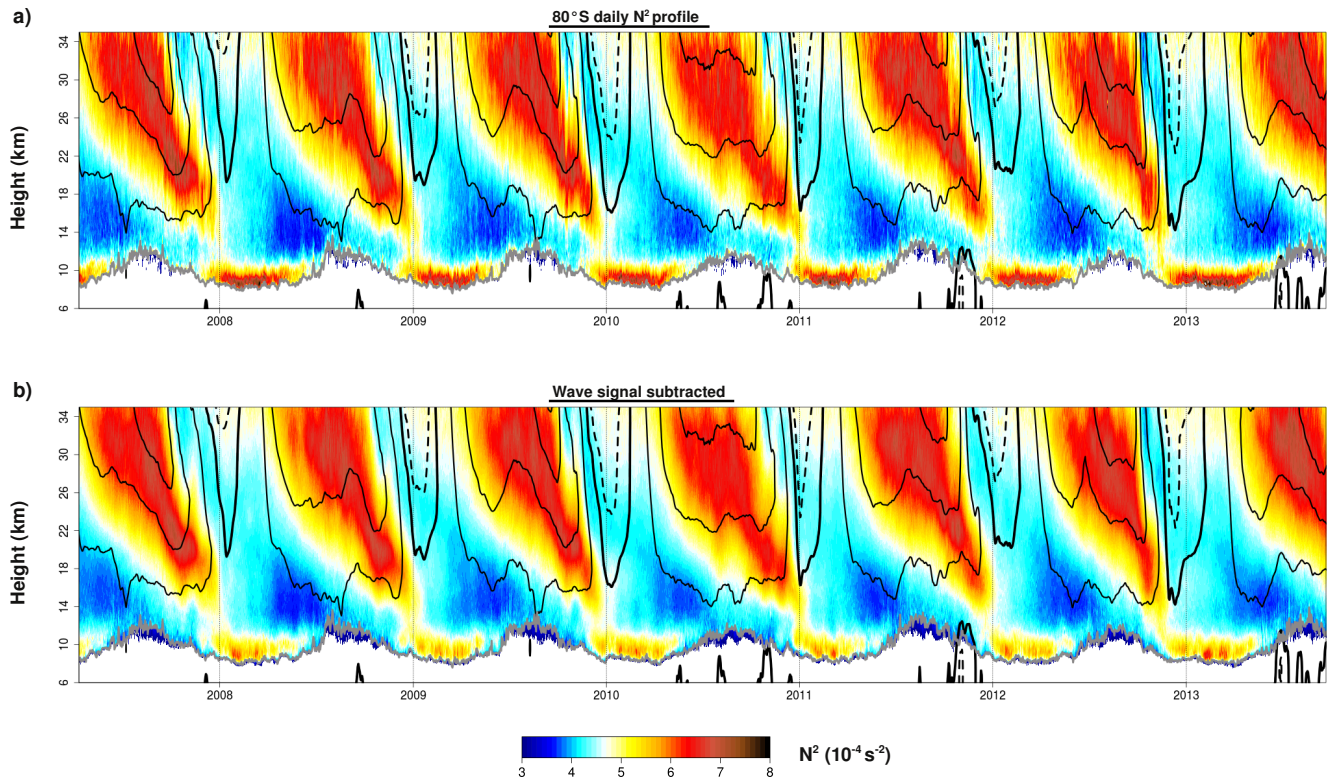


**Figure 9.** As in Fig. 5 and 7, but for 80°S. First easterly wind contour (dashed line) at -3m/s for better visibility. The rest of wind contours are 10m/s intervals as in Fig. 5.

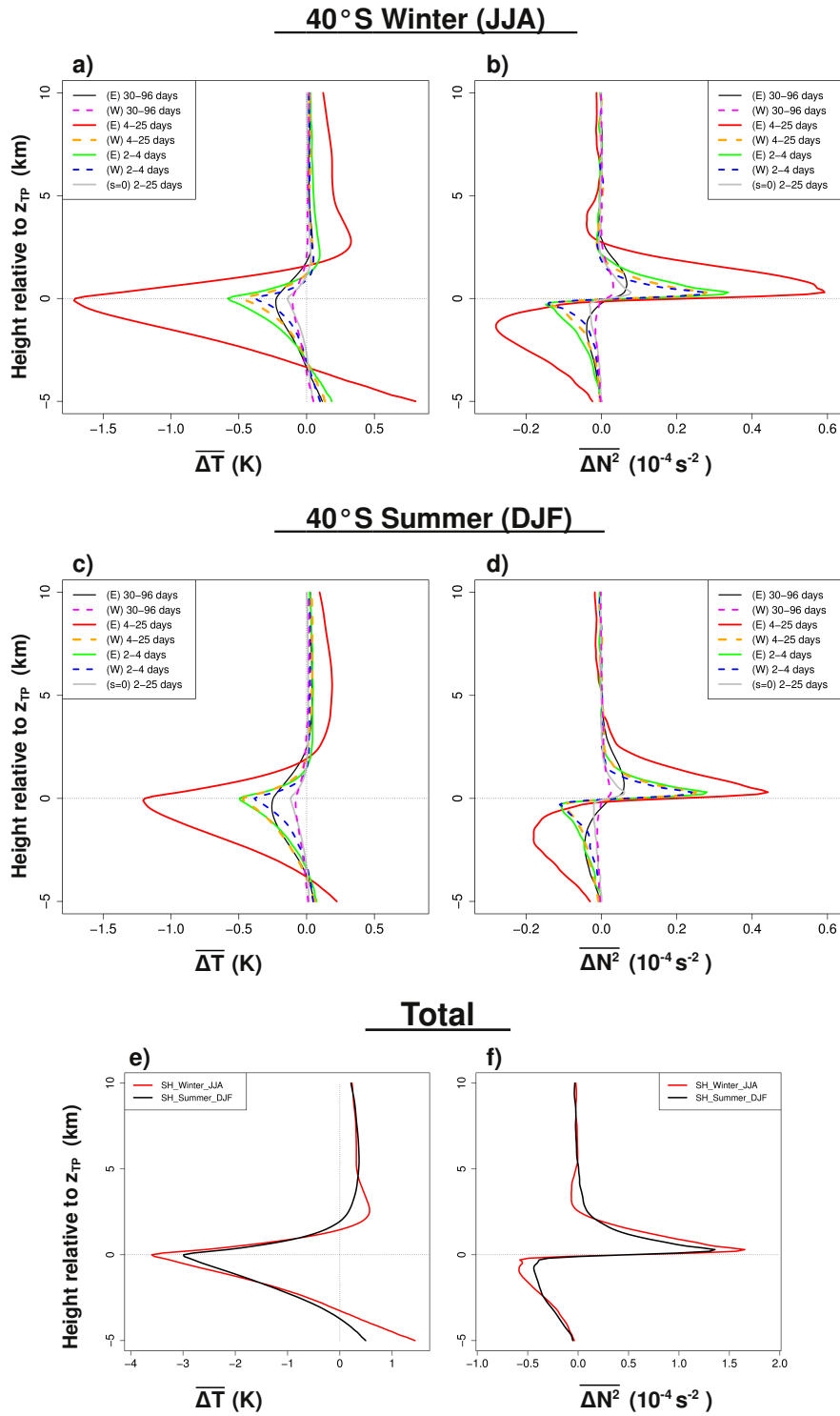


**Figure A1.** As in Figs. 4, 6 and 8, but for 40°S.

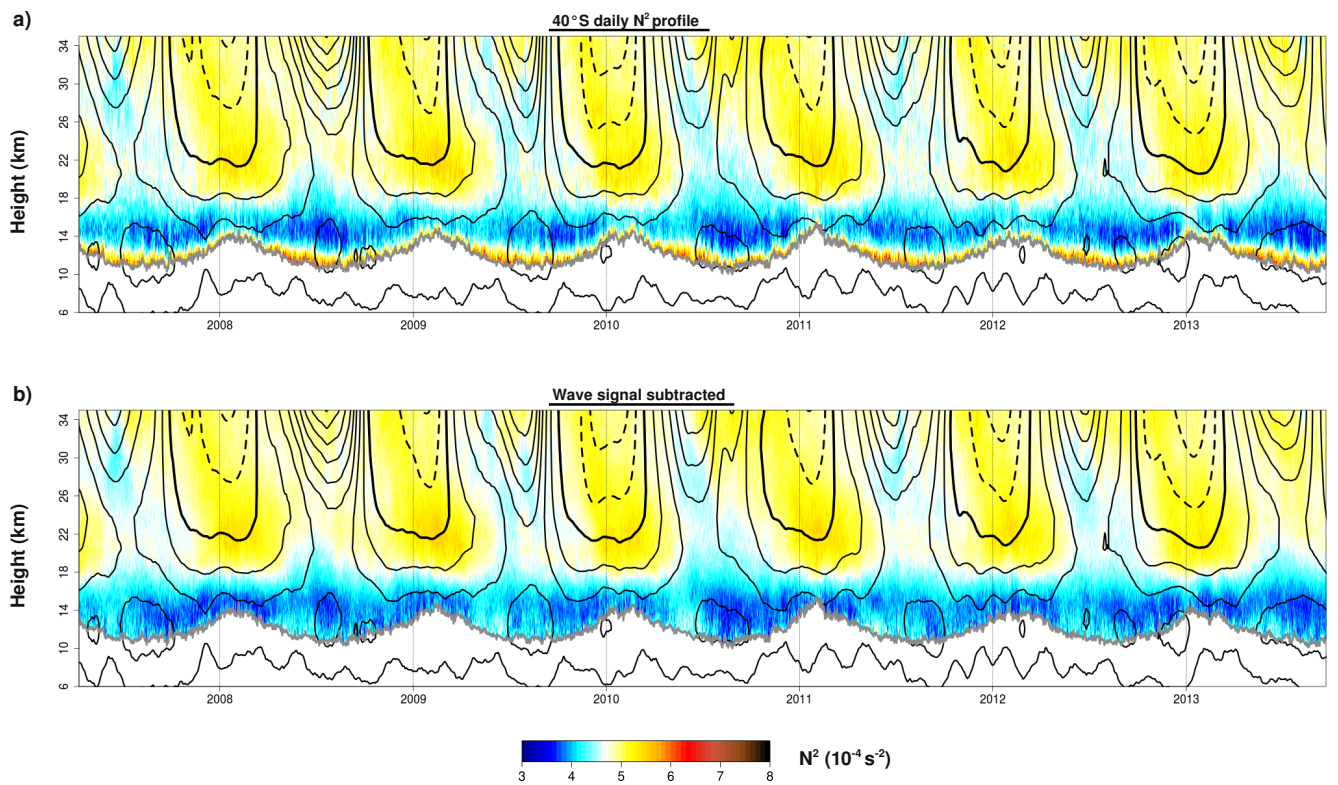


Figure A2. As in Fig. 5, but for 40°S.